July 5, 1973

To the Graduate Council:

I am submitting herewith a thesis written by I-lan Tang entitled "Optical Properties of Nucleic Acid Bases." I recommend that it be accepted for nine quarter hours of credit in partial fulfillment of the requirements for the degree of Master of Science, with a major in Physics.

R. D. Lovell
Major Professor

We have read this thesis
and recommend its acceptance:

Robert W. Lide

R. O. Bickhoff

Accepted for the Council:

Hilton A. Smith
Vice Chancellor for
Graduate Studies and Research

OPTICAL PROPERTIES OF NUCLEIC ACID BASES

A Thesis

Presented to

the Graduate Council of

The University of Tennessee

In Partial Fulfillment

of the Requirements for the Degree

Master of Science

---

by

I-lan Tang

August 1973

ACKNOWLEDGMENTS

The author would like to thank Drs. E. T. Arakawa, M. W. Williams, and R. N. Hamm for many helpful discussions, for computer programming assistance by Dr. Hamm, for experimental assistance by Dr. L. C. Emerson, and for the constant encouragement and guidance by Dr. R. D. Birkhoff.

This research was supported by the Oak Ridge National Laboratory which is operated by Union Carbide Corporation for the U.S. Atomic Energy Commission.

1104225

ABSTRACT

The optical properties are reported for the nucleic acid bases adenine, thymine, cytosine, and guanine in the energy range from 4 to 10 eV. Thin films of these bases were sublimed onto CaF_2 or glass in vacuum, exposed to the atmosphere while being transferred to the reflectometer, and measured with the films maintained in vacuum. The imaginary part of the refractive index, k, was determined from measurements of transmittance as a function of film thickness for each experimental wavelength. There is virtually no experimental scatter associated with the k data for a given film, but the magnitude of k is not reproducible from one film to another especially in the shorter wavelength region. Inhomogeneities in the films, surface irregularities, and contamination are some of the factors that could be involved. Further experimentation on conditions affecting film structure must be done. Representive k values obtained from transmission measurements combined with the measured reflectance at 20° photon angle of incidence were then used to calculate n, the real part of the refractive index as a function of wavelength. The dielectric constant, $\varepsilon = \varepsilon_1 + i\varepsilon_2$, and the energy loss function, $-\mathrm{Im}(1/\varepsilon)$, were then calculated from the n and k values by the relations $\varepsilon_1 = n^2 - k^2$, $\varepsilon_2 = 2nk$, and $-\mathrm{Im}(1/\varepsilon) = \varepsilon_2/(\varepsilon_1^2 + \varepsilon_2^2)$. The energy loss function calculated from the optical constants enables us to compare directly with the energy loss spectra of 25 keV electrons passing through thin films of nucleic acid bases reported in the literature. It was found that there is fair agreement between the structure in $-\mathrm{Im}(1/\varepsilon)$ and the structure in the electron energy loss spectra.

Structure in ε_2 and $-\mathrm{Im}(1/\varepsilon)$ as a function of photon energy was interpreted in terms of $\pi \rightarrow \pi^*$ molecular excitations and collective oscillations.

TABLE OF CONTENTS

CHAPTER		PAGE
I.	INTRODUCTION	1
	Introduction	1
	Review of Previous Work	4
	Present Work	5
II.	THEORY	7
	Optical Constants	7
	Reflectance	9
	Transmittance	12
	Energy loss function	13
	Classical Dielectric Theory	14
	Covalent Bonding	17
III.	EXPERIMENTAL APPARATUS	20
	Apparatus for Evaporation	20
	Apparatus for Measuring Optical Properties	20
IV.	EXPERIMENTAL PROCEDURE AND DETERMINATION OF OPTICAL CONSTANTS	24
	Substrate Cleaning	24
	Film Preparation	24
	Transmission Measurements	31
	Reflectance Measurements	33
V.	RESULTS AND DISCUSSION	35
	Optical Constants	35
	Optical Properties	44

CHAPTER PAGE

VI. SUMMARY 54

BIBLIOGRAPHY 56

VITA 59

LIST OF TABLES

TABLE PAGE

1. Evaporation conditions for making nucleic acid bases films 26

2. Comparison of the sublimation temperatures of the nucleic acid bases 28

3. Comparison of the positions of the absorption peaks for sublimed nucleic acid bases films 29

4. Comparison of the positions of the peaks in $-Im(1/\varepsilon)$ from both electron energy loss and optical measurements, in ε_2 and in the absorption coefficient μ for sublimed films 50

LIST OF FIGURES

FIGURE		PAGE
1.	Molecular structure of the nucleic acid bases	2
2.	Structure of DNA	3
3.	Schematic diagram of a planar thin film of thickness d and infinite area bounded on either side by semi-infinite media	10
4.	Behavior of the real and imaginary parts of the dielectric constant and the energy loss function for a) Drude's ($\hbar\omega_p$ = 20 eV and $\hbar\gamma$ = 2 eV) and b) Lorentz's model ($\hbar\omega_p$ = 20 eV, $\hbar\omega_o$ = 10 eV, and $\hbar\gamma$ = 2 eV)	16
5.	Schematic diagram, top view, of the experimental apparatus for measuring the optical properties	22
6.	Transmission of adenine from films of four different thicknesses	32
7.	Extinction coefficient, k, of adenine as a function of wavelength	36
8.	Extinction coefficient, k, of thymine as a function of wavelength	37
9.	Extinction coefficient, k, of cytosine as a function of wavelength	38
10.	Extinction coefficient, k, of guanine as a function of wavelength	39
11.	Reflectance, R, and index of refraction, n, of adenine as a function of wavelength	40

FIGURE PAGE

12. Reflectance, R, and index of refraction, n, of thymine as a function of wavelength 41

13. Reflectance, R, and index of refraction, n, of cytosine as a function of wavelength 42

14. Reflectance, R, and index of refraction, n, of guanine as a function of wavelength 43

15. Dielectric constants, ε_1 and ε_2, and energy loss function, $-\mathrm{Im}(1/\varepsilon)$, of adenine as a function of photon energy 45

16. Dielectric constants, ε_1 and ε_2, and energy loss function, $-\mathrm{Im}(1/\varepsilon)$, of thymine as a function of photon energy 46

17. Dielectric constants, ε_1 and ε_2, and energy loss function, $-\mathrm{Im}(1/\varepsilon)$, of cytosine as a function of photon energy 47

18. Dielectric constants, ε_1 and ε_2, and energy loss functions, $-\mathrm{Im}(1/\varepsilon)$, of guanine as a function of photon energy 48

CHAPTER I

INTRODUCTION

I. Introduction

The cell is the basic unit for living organisms. The genetic material of the cell constitutes the basic input of information that determines the activities of the cell. It is composed of very long DNA molecules surrounded by a protein coat. Every DNA molecule is comprised of many nucleotides linked in one long chain. Each nucleotide contains a phosphate group, a pentose sugar (one that contains five carbon atoms), and an organic base. Four kinds of bases are found in DNA, i.e., adenine, thymine, guanine, and cytosine. Their structures are shown in Figure 1.

The DNA molecule is composed of two chains of nucleotides spiraling around a common center to form a double helix. Its structure is shown in Figure 2. The bases of one chain are bonded by hydrogen bonds to the bases of the other chain. These bonds are formed only between specific pairs of bases. Adenine, in one chain, is always bonded to thymine in the other chain, and cytosine is always bonded to guanine. Because the bases will pair in only one way, the sequence of bases in one chain determines the sequence of bases in the other. The genetic information is determined by the various sequences. This model of DNA was proposed by Watson and Crick (1971).

There have been speculations that quantum electronic properties of DNA macromolecules may be directly related to their biological functions. Theoretical calculations of the spectral properties of DNA have been done by Rhodes (1961), Ladik (1971), Pullman et al. (1969), Fenton (1965),

ORNL DWG. 73-5001

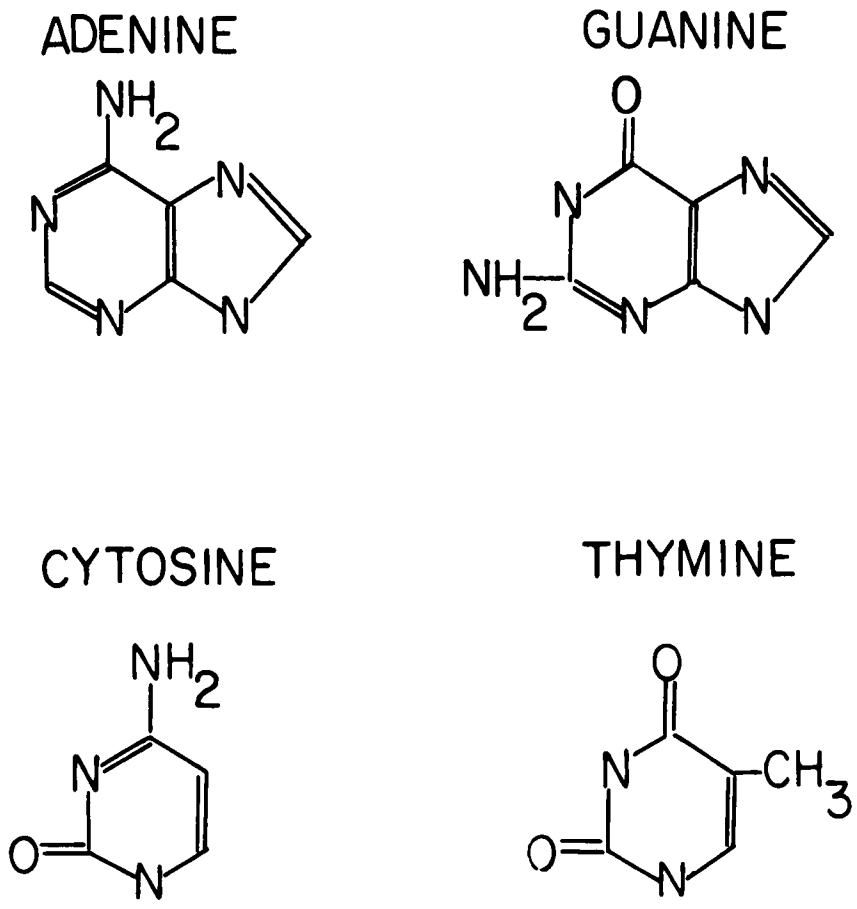


Figure 1. Molecular structure of the nucleic acid bases.

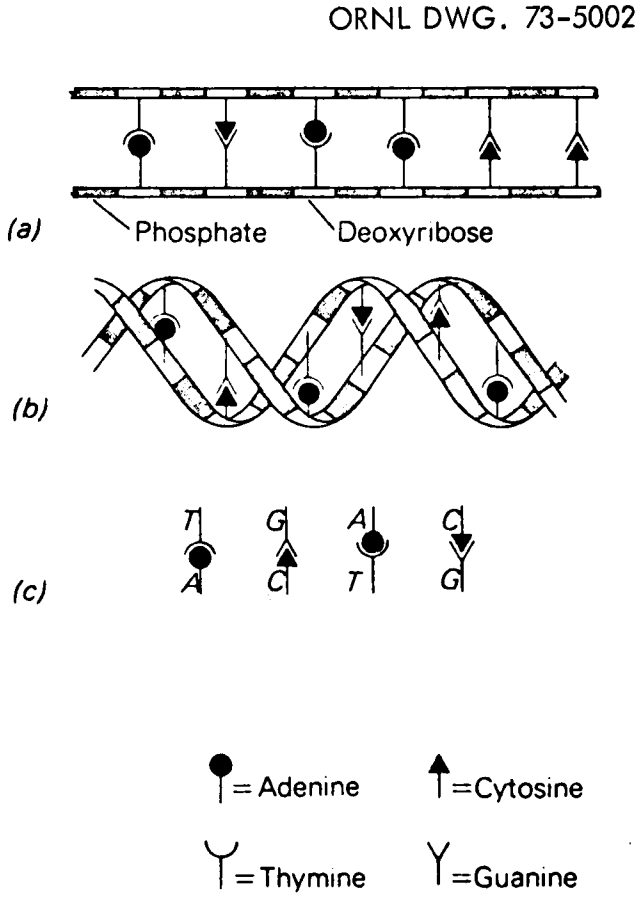


Figure 2. Structure of DNA.

a) Nitrogen bases link alternate phosphate and deoxyribose groups. b) The double helix. c) The pairing of the bases.

and Hoffman et al. (1964). Experimental work on the conductivity and dielectric constants of DNA and related compounds have been done by Weissbluth (1971), O'Konski et al. (1970), and Snart (1968). There is still no satisfactory electronic structure for DNA.

The electron energy loss measurements for the bases obtained using a scanning electron microscope equipped with a high resolution magnetic spectrometer have been reported by Johnson (1972) and Isaacson (1972). Eventually the aim is to refine this method so that the sequence of bases in a particular DNA molecule can be identified from the spectra of the individual bases. It has been thought that the results obtained might be affected by radiation damage done to the DNA molecule by the scanning electron beam. As a check on this, we have initiated a study of the optical properties of the nucleic acid bases which will enable us to calculate the energy loss functions which can be compared directly with the measured electron energy loss spectra.

II. Review of Previous Work

Most of the spectral studies on nucleic acid bases were done in the near UV region where the well known 2600 Å band exists. Voet et al. (1963) extended measurements down to 1850 Å, and Yamada et al. (1968) extended them further to 1200 Å. Different bases show different absorption characteristics. The energy loss spectra of 25 keV electrons passing through thin films of the nucleic acid bases were measured by Johnson (1972) and Isaacson (1972) over the range of energy losses from 0 to 500 eV. Transitions from π and σ molecular orbital levels as well as K atomic levels to bound excited states were discussed. Collective effects were also observed.

III. Present Work

Techniques and theories involving the determination of the electronic properties of solids from optical methods in the vacuum UV region have been developed in recent years. The optical properties can be specified by the optical constants, n and k, the real and imaginary parts of the complex index of refraction, respectively. These parameters can then be used to calculate the complex dielectric constant, $\varepsilon = \varepsilon_1 + i\varepsilon_2$, and the energy loss function $-\mathrm{Im}(1/\varepsilon)$.

The nucleic acid bases were sublimed in vacuum on glass slides and CaF_2 discs for reflectance and transmission measurements, respectively. Appropriate sublimation temperatures were used for each of the bases. The film thickness was measured with a thickness monitor set in the vacuum chamber.

Reflectance and transmission measurements were made from 1250 Å to 3200 Å to determine the optical constants for four nucleic acid bases. The complex dielectric constant and the energy loss function were then calculated from the optical constants. The quantity ε_2 is directly proportional to the dissipation of electromagnetic energy in the medium. It has a pronounced structure and peaks where certain excitations of electrons, e.g., molecular excitations or single electron transitions, occur with high probability. The probability that an electron passing through a solid will lose an amount of energy equal to $\hbar\omega$ is related to $-\mathrm{Im}\ 1/\varepsilon$ [Ritchie (1957)]. This quantity enables us to compare the energy loss spectra obtained for fast electrons with the results of the optical methods. In this work, the positions of the absorption peaks were also compared with Yamada and Fukutome's (1968)

optical data from 1250 Å to 3000 Å. The data were then interpreted in terms of molecular excitations and collective effects in the molecules.

CHAPTER II

THEORY

I. Optical Constants

When electromagnetic radiation is incident on a boundary separating two different media, part of it is reflected, and part of it is transmitted into the second medium. The amount of radiation that is reflected or transmitted is determined by the optical properties of the medium. The optical properties can be characterized by the optical constants, n and k, the real and imaginary parts, respectively, of the complex index of refraction $\tilde{n}$, where n, the index of refraction, is defined as the ratio of the velocity of the radiation in vacuum to its phase velocity in the medium, $n = c/v$, and k is often referred to as the extinction coefficient.

For a plane electromagnetic wave traveling in the positive z direction in an absorbing medium the equations for the amplitudes of the electric and magnetic fields can be written as

$$\vec{E} = \vec{E}_o \exp\left[i\left(\frac{2\pi n}{\lambda} z - \omega t\right)\right] \exp\left[-\frac{2\pi k}{\lambda} z\right] \qquad (1)$$

$$\vec{H} = \vec{H}_o \exp\left[i\left(\frac{2\pi n}{\lambda} z - \omega t\right)\right] \exp\left[-\frac{2\pi k}{\lambda} z\right] \qquad (2)$$

where z is the distance and t is the time of propagation of the wave through the medium, $\vec{E}_o$ and $\vec{H}_o$ are the electric and magnetic field intensities at $z = 0$ and $t = 0$, ω is the frequency, and λ is the wavelength in vacuum. The problem of determining the amount of light reflected and transmitted by an optical system may be solved by using Maxwell's equations with suitable boundary conditions. For an isotropic medium with

zero charge density and negligible magnetic susceptibility, Maxwell's equations can be written

$$\nabla \cdot \vec{E} = 0 , \tag{3}$$

$$\nabla \cdot \vec{H} = 0 , \tag{4}$$

$$\nabla \times \vec{E} = \frac{-1}{c} \frac{\partial \vec{H}}{\partial t} , \tag{5}$$

$$\nabla \times \vec{H} = \frac{\varepsilon}{c} \frac{\partial \vec{E}}{\partial t} . \tag{6}$$

The dielectric constant, ε, is a complex quantity with real and imaginary parts ε_1 and ε_2, respectively. Equation (5) can be solved for $\vec{E}$ by taking the curl of Equation (5) and substituting for $\nabla \times \vec{H}$ from Equation (6) giving

$$\nabla^2 \vec{E} = \frac{\varepsilon}{c^2} \frac{\partial^2 \vec{E}}{\partial t^2} \tag{7}$$

and similarly for the magnetic vector

$$\nabla^2 \vec{H} = \frac{\varepsilon}{c^2} \frac{\partial^2 \vec{H}}{\partial t^2} . \tag{8}$$

Substituting Equation (1) into Equation (7) shows that

$$\varepsilon = \tilde{n}^2 \tag{9}$$

so the dielectric constants, ε_1 and ε_2, are related to the optical constants, n and k, by

$$\varepsilon_1 = n^2 - k^2 \tag{10}$$

$$\varepsilon_2 = 2nk . \tag{11}$$

Hence the measurements of n and k give ε_1 and ε_2. Both ε and $\tilde{n}$ contain the same physical information. For purposes of theoretical descriptions, the dielectric constants turn out to be more convenient.

Reflectance

Consider a planar thin film of thickness d and infinite area bounded on either side by semi-infinite non-absorbing media as shown in Figure 3. Let medium 0 have index of refraction n_o, and the semi-infinite substrate described by medium 2 have index of refraction n_2. Both media 0 and 2 are transparent, i.e., $k_o = 0$ and $k_2 = 0$. The thin film is described by medium 1 with optical constants n_1 and k_1. Let the light be incident through medium 0 at an angle of incidence ϕ_o with respect to the normal to the interface between media 0 and 1. Since the incident light is partially polarized, both components must be treated. Let subscript s denote the electric vector perpendicular to the plane of incidence and p denote the electric vector parallel to the plane of incidence. Then the amplitudes of the reflected and transmitted components are

$$r_{1p} = \frac{\sigma_1 - \varepsilon_1\mu}{\sigma_1 + \varepsilon_1\mu} \tag{12}$$

$$r_{2p} = \frac{\varepsilon_1\sigma_2 - \varepsilon_2\sigma_1}{\varepsilon_1\sigma_2 + \varepsilon_2\sigma_1} \tag{13}$$

$$t_{1p} = \frac{2\mu\tilde{n}_1}{\sigma_1 + \varepsilon_1\mu} \tag{14}$$

$$t_{1p'} = \frac{2\sigma_1\,\tilde{n}_1}{\sigma_1 + \varepsilon_1\mu} \tag{15}$$

$$r_{1s} = \frac{\mu - \sigma_1}{\mu + \sigma_1} \tag{16}$$

$$r_{2s} = \frac{\sigma_1 - \sigma_2}{\sigma_1 + \sigma_2} \tag{17}$$

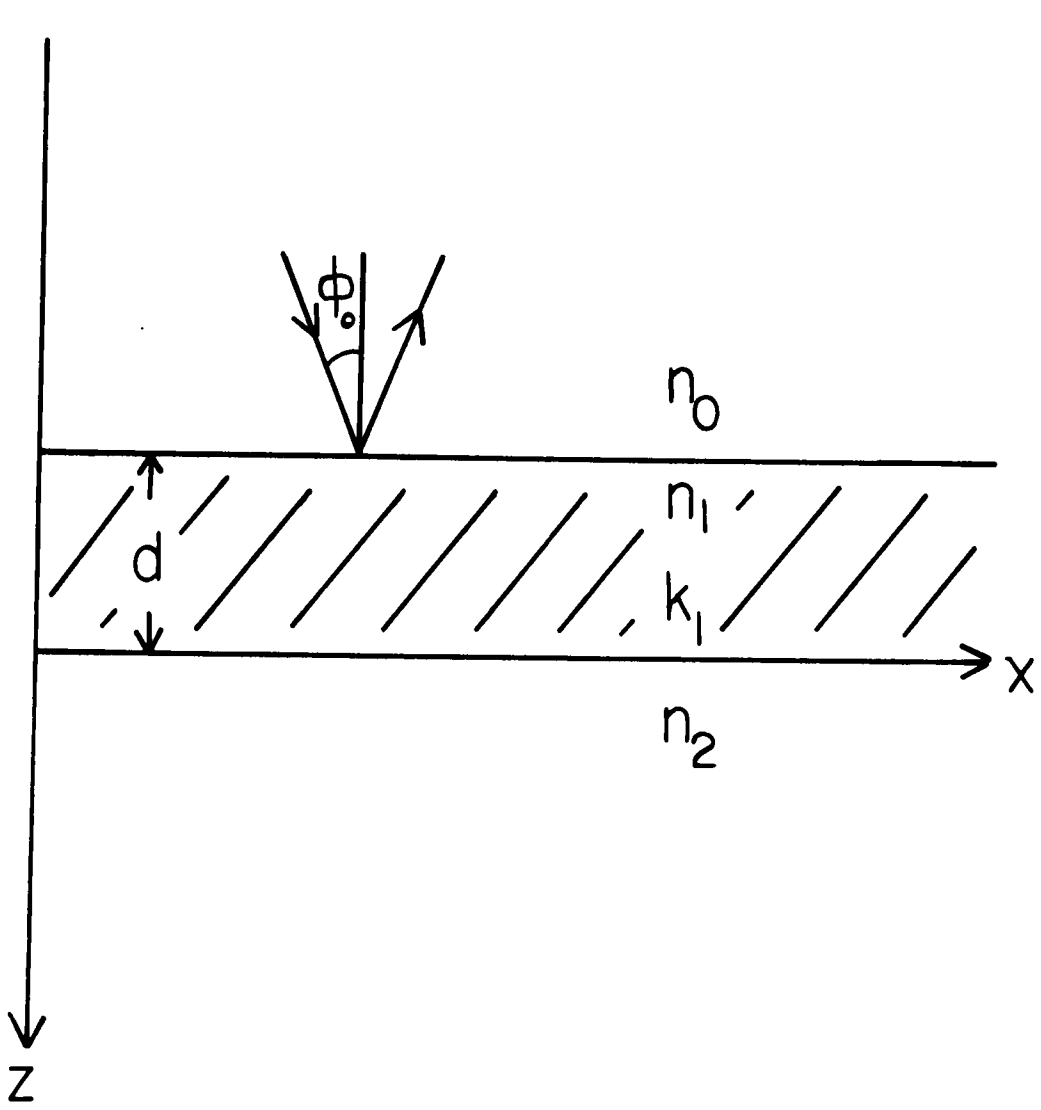


Figure 3. Schematic diagram of a planar thin film of thickness d and infinite area bounded on either side by semi-infinite media.

$$t_{1s} = \frac{2\mu}{\mu + \sigma_1} \tag{18}$$

$$t_{1s'} = \frac{\sigma_1}{\mu + \sigma_1} \tag{19}$$

where r_{1p} and r_{1s} are the amplitudes of the parallel and perpendicularly polarized light reflected from the interface between media 0 and 1, respectively, r_{2p} and r_{2s} are the amplitudes of the parallel and perpendicularly polarized light reflected from the interface between media 1 and 2, respectively, t_{1p} and t_{1s} are the amplitudes of the parallel and perpendicularly polarized light transmitted from medium 0 to medium 1, respectively, and $t_{1p'}$ and $t_{1s'}$ are the amplitudes of the parallel and perpendicularly polarized light transmitted from medium 1 to 0 after it is reflected from the interface between media 1 and 2, respectively. $\tilde{n}_1$, $\tilde{n}_2$, ε_1, ε_2, σ_1, σ_2, μ, and δ are defined as

$$\tilde{n}_1 = \frac{n_1 + ik_1}{n_o} \tag{20}$$

$$\tilde{n}_2 = \frac{n_2}{n_o} \tag{21}$$

$$\varepsilon_1 = \tilde{n}_1^2 \tag{22}$$

$$\varepsilon_2 = \tilde{n}_2^2 \tag{23}$$

$$\sigma_1 = \sqrt{\varepsilon_1 - \sin^2\phi_o} \tag{24}$$

$$\sigma_2 = \sqrt{\varepsilon_2 - \sin^2\phi_o} \tag{25}$$

$$\mu = \cos\phi_o \tag{26}$$

and

$$\delta = \frac{2\pi d}{\lambda} n_o \sigma_1 \ . \tag{27}$$

Then the amplitude of the light reflected by this system is given by

$$r_i = r_{1i} + \frac{t_{1i} t_{1i'} r_{2i} e^{2i\delta}}{1 + r_{1i} r_{2i} e^{2i\delta}} \tag{28}$$

where i = p, s. The reflectance of this system is given by

$$R = \frac{|r_s|^2 + P|r_p|^2}{1 + P} \tag{29}$$

where

$$P = \frac{I_P}{I_S} \tag{30}$$

is the ratio of the light intensity polarized parallel to the plane of incidence to that polarized perpendicular to the plane of incidence. In this investigation Equation (29) is used in two ways. For each λ, (1) measurement of R at a known angle of incidence together with independent measurements of d, k, and P yields a calculated value of n and (2) measurement of R as a function of angle of incidence together with independent measurements of d and P yields values of n and k.

Transmittance

Consider light incident normally, i.e., $\phi = 0$ in Figure 3, page 10. The amount of light absorbed by the film can be found by measuring the reduction in the incident light intensity after it has traversed a thickness d of the material. In this way the optical extinction coefficient can be determined independently of the reflectance measurements. The intensity of a wave propagating through an absorbing medium is given by

the time-averaged Poynting vector which is equal to $(c/8\pi)(\vec{E} \times \vec{H})$. Use of Equations (1) and (2) in this expression gives

$$I = I_o \exp - (4\pi kd/\lambda) \tag{31}$$

where I_o is the intensity at $z = 0$ and I is the intensity of the wave after traveling a distance d through the medium in the direction of propagation of the wave. If Equation (31) is compared with the Lambert-Beer law

$$I = I_o \exp [-\alpha d] \tag{32}$$

where α is defined as the optical absorption coefficient, the imaginary part of the complex index of refraction is related to the absorption coefficient by

$$\alpha = \frac{4\pi k}{\lambda} . \tag{33}$$

Energy Loss Function

The probability that a fast, charged particle traversing a solid will lose an amount of energy equal to $\hbar\omega$ was shown by Ritchie (1957) to be related to the function $-\mathrm{Im}(1/\varepsilon)$. In terms of the real and imaginary parts of the dielectric constant of the medium, this energy loss function is

$$-\mathrm{Im}(1/\varepsilon) = \frac{\varepsilon_2}{\varepsilon_1^2 + \varepsilon_2^2} . \tag{34}$$

Thus if the optical and dielectric constants are obtained for a medium from measurements of reflectance and transmittance, the energy loss function can be calculated from Equation (34). This can be compared with electron energy loss measurements for the same material.

II. Classical Dielectric Theory

The distinction between metals and insulators is frequently based upon their responses to the dc electric field. However, the optical properties of metals and insulators have much in common in the ultraviolet. The model that the electrons in a metal form a gas of free particles was proposed by Drude. An equally simple picture for insulators was proposed by Lorentz. In this case the electrons can be envisioned as tied to certain equilibrium positions by springs.

The response of one of the electrons of mass m and charge -e, in a Lorentz insulator to a uniform oscillating electric field, $\vec{E} = \vec{E}_o e^{-i\omega t}$, is described by the equation of motion

$$\frac{d^2\vec{X}}{dt^2} + \gamma \frac{d\vec{X}}{dt} + \omega_o^2 \vec{X} = \frac{-e\vec{E}}{m} . \tag{35}$$

Here $\gamma \frac{d\vec{X}}{dt}$ is the damping term proportional to the velocity and characterized by a damping constant γ, ω_o is the natural frequency associated with Hooke's Law describing the restoring force of a spring, and the right hand side of the equation represents the driving term due to the electric field.

Since the equation is linear in the displacement X, we may assume that it has the same time dependence as $\vec{E}$. Then the displacement is

$$\vec{X} = \frac{-e\vec{E}}{m[\omega_o^2 - \omega^2 + i\gamma\omega]} . \tag{36}$$

For a dielectric material with N electrons per unit volume the polarization is defined as

$$\vec{P} = -Ne\vec{X} \tag{37}$$

and is related to the electric field by

$$\vec{P} = \frac{(\varepsilon - 1)}{4\pi} \vec{E} \ . \tag{38}$$

Thus from Equations (36) and (37) the polarization can be written as

$$\vec{P} = \frac{Ne^2\vec{E}}{m(\omega_o^2 - \omega^2 + i\gamma\omega)} \ . \tag{39}$$

Substitution of Equation (39) into Equation (38) yields

$$\varepsilon = 1 - \frac{4\pi Ne^2/m}{(\omega_o^2 - \omega^2 + i\gamma\omega)} \ . \tag{40}$$

The real and imaginary parts of the dielectric constant, ε_1 and ε_2, can be written respectively as

$$\varepsilon_1 = 1 + \left(\frac{4\pi Ne^2}{m}\right)\left(\frac{(\omega_o^2 - \omega^2)}{(\omega_o^2 - \omega^2)^2 + \gamma^2\omega^2}\right) \tag{41}$$

$$\varepsilon_2 = \left(\frac{4\pi Ne^2}{m}\right)\left(\frac{\gamma\omega}{(\omega_o^2 - \omega^2)^2 + \gamma^2\omega^2}\right). \tag{42}$$

The behavior for the real and imaginary parts of the dielectric constants for both Lorentz's and Drude's models are shown in Figure 4, and it is seen that at sufficiently high energies the dielectric response is very similar in metals and insulators. The energy loss function $[-\mathrm{Im}(1/\varepsilon)]$ calculated for the given values of ε_1 and ε_2 are also shown. The dissipation of electromagnetic energy in the medium is given by [Kloos (1968)]

$$\frac{dW}{dt} = \varepsilon_2\omega\vec{E}^2 \tag{43}$$

where $\vec{E}$ is the electric field of the photon. Thus, ε_2 should show structure where certain excitations of electrons occur with high probability,

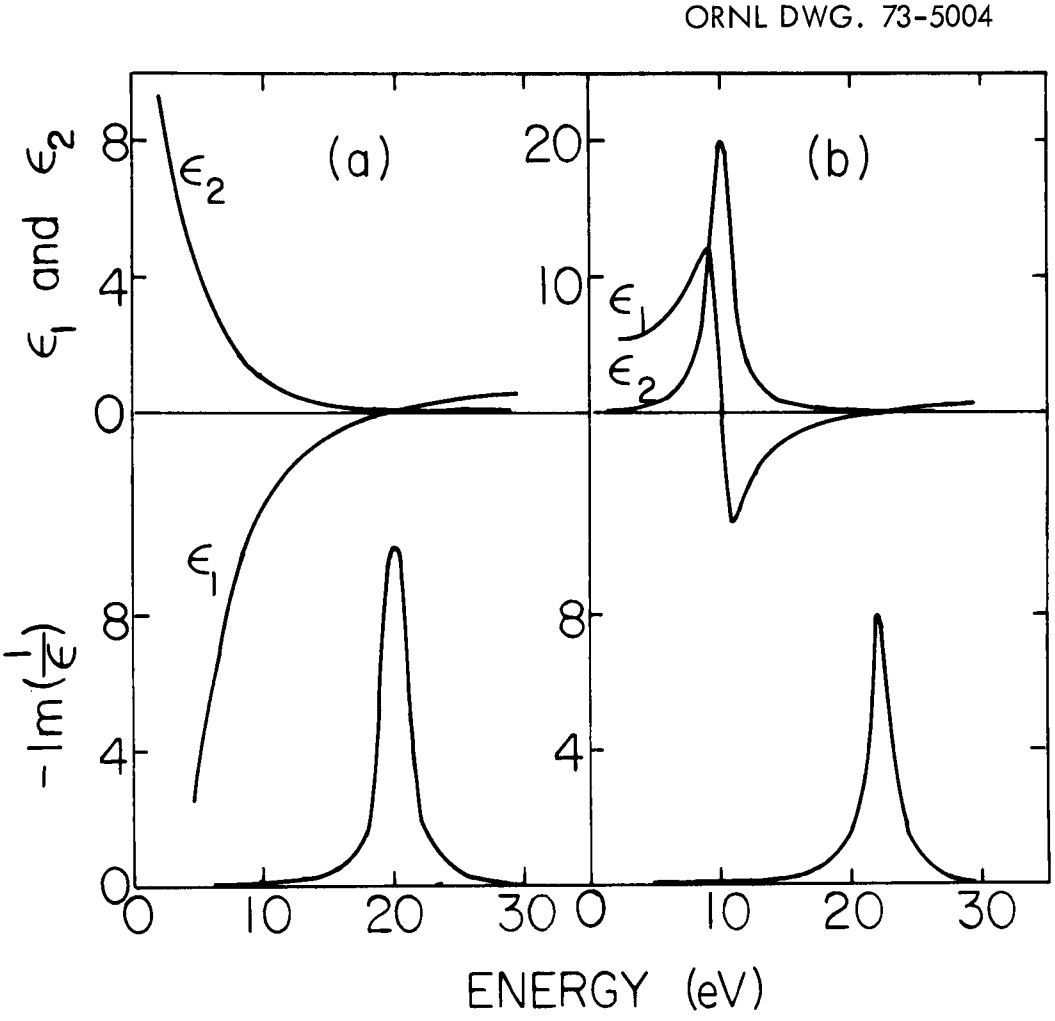


Figure 4. Behavior of the real and imaginary parts of the dielectric constant and the energy loss function for a) Drude's ($\hbar\omega_p$ = 20 eV and $\hbar\gamma$ = 2 eV) and b) Lorentz's model ($\hbar\omega_p$ = 20 eV, $\hbar\omega_o$ = 10 eV, and $\hbar\gamma$ = 2 eV).

and the theoretical band structure can be checked by comparing it with the spectral dependence of ε_2.

The condition for the existence of collective oscillations is that the complex dielectric constant $\varepsilon = 0$. In practice, it is not necessary to require that $\varepsilon_1 = 0$ in the region where $\varepsilon = 0$. It has been shown that the maximum of $-\mathrm{Im}(1/\varepsilon)$ corresponds to a collective resonance if ε_1 and ε_2 are (i) small in the region of the peak, (ii) approximately linearly varying with $d\varepsilon_1/d\omega > 0$ and $d\varepsilon_2/d\omega < 0$ and (iii) $(\omega/\varepsilon_1)\, d\varepsilon_1/d\omega$ and $(\omega/\varepsilon_2)\, d\varepsilon_2/d\omega >> 1$ [Ehrenreich and Phillipp (1962)]. It is shown by Powell (1969) that it is difficult to correlate maxima in $-\mathrm{Im}(1/\varepsilon)$ with maxima in ε_2 and to identify a particular maximum in $-\mathrm{Im}(1/\varepsilon)$ as being associated with a volume plasmon excitation. Maxima in $-\mathrm{Im}(1/\varepsilon)$ may occur at substantially different frequencies and with differing relative intensities than maxima in ε_2. The calculations in this paper show that both the positions and the intensities of structure in $-\mathrm{Im}(1/\varepsilon)$ can be strongly influenced by the combination of the several contributions to $\varepsilon(\omega)$.

III. Covalent Bonding

In order to interpret the structure of the organic compounds from the optical data, a brief description of the molecular orbital picture and covalent bonding is given in this section.

Atoms are held together in a molecule by chemical bonds. There are usually two kinds of bonding in molecules, the ionic bond and the covalent bond. The ionic bond results from the transfer of electrons, while the covalent bond results from sharing of electrons. Covalent bonding is the more important in organic molecules.

A carbon atom forms four covalent bonds with other atoms by promoting one of its 2s electrons to the vacant 2p orbital and the four orbitals hybridize to form four sp^3 orbitals. In some molecules with a carbon-carbon bond three hybrid sp^2 orbitals form bonds with three other atoms such as hydrogen. These sp^2 orbitals lie in one plane and form bonds which are cylindrically symmetrical about a line joining the nuclei. These are called σ bonds. The remaining p orbital consists of two equal lobes, one lying above and the other lying below the plane of the three sp^2 orbitals, and is occupied by a single electron. If this p orbital of one carbon atom overlaps the p orbital of another carbon atom, the electrons pair up and an additional bond, called a π-bond, is formed. The π-bond thus consists of two parts, one electron cloud lies above the plane of the atoms and another electron cloud lies below. π bonds are weaker than σ bonds because of less overlapping. Similarly in a benzene ring, three sp^2 orbitals are used for each carbon atom to form a hexagon. All the atoms of benzene lie in one plane. Hence as before, these bonds are σ bonds. The remaining p orbital of each carbon atom overlaps the p orbital of an adjacent carbon atom, and a π bond is formed. But the overlapping is not limited to a pair of p orbitals. The p orbital of any one carbon atom overlaps equally well the p orbitals of both carbon atoms to which it is bonded. The result is two continuous doughnut-shaped electron clouds, one lying above and one lying below the plane of the C_6H_6 molecule. Overlapping of atomic orbitals can also result in an electron density between the atomic nuclei which is less than that at the same distance from the nucleus in an isolated atom. These states are called antibonding and

are designated as σ^* and π^*. They are less stable than the corresponding bonding states and hence have higher energies. There are unshared electrons or non-bonded electrons in molecules containing atoms like nitrogen, oxygen, etc. They are usually called n-electrons and are less tightly bound to the molecule than the σ and π electrons. In general the $n \rightarrow \pi^*$ transitions require the smallest energy followed by $n \rightarrow \sigma^*$, $\pi \rightarrow \pi^*$, and $\sigma \rightarrow \sigma^*$ in that order. The $n \rightarrow \pi^*$ and $n \rightarrow \sigma^*$ transitions are usually found in the visible through the near ultraviolet. The $\pi \rightarrow \pi^*$ transitions are observed in the ultraviolet through the vacuum ultraviolet and the $\sigma \rightarrow \sigma^*$ transitions only in the vacuum ultraviolet.

The above picture only provides a qualitative description of the processes involved in molecular bonding for organic compounds. For a particular molecule and its energy transitions, detailed calculations must be used to account for all the processes of molecular bonding.

CHAPTER III

EXPERIMENTAL APPARATUS

The experiment involves two pieces of apparatus. One is for the evaporation of nucleic acid bases to make thin films on the substrate. The other is for the measurement of the optical properties of these bases. They are described separately as follows:

I. Apparatus for Evaporation

The basic apparatus consists of a vacuum system, a coating chamber, a thickness monitor (Kronos Model QM-2), and a digital temperature indicator (Newport Series 260, Type K). The vacuum system consists of a mechanical pump, an oil diffusion pump, and a liquid nitrogen cold trap. This liquid nitrogen cold trap is used to reduce contamination due to diffusion pump oil in the high vacuum system. The nucleic acid bases were put on a flat tantalum boat which was clamped to the electrodes which were in turn connected to a low voltage power supply. The reasons for using tantalum as the source heater are mainly because of its low vapor pressure at high temperature and its high melting point. The thermocouple of the temperature indicator was put on the edge of the boat at its center. The thickness monitor was set with the same relative geometry to the boat as the substrate in order to get the right reading of the thickness of the film.

II. Aparatus for Measuring the Optical Properties

The apparatus was designed to measure the optical properties of thin films in the region from 6500 to 1160 Å or approximately 2.0 to

10.6 eV. The basic experimental apparatus consists of a source of electromagnetic radiation, a dispersive grating, a reflectance chamber, a beam monitor, and associated electronic equipment capable of detecting small currents. All the equipment was already in existence at the beginning of this work. The schematic diagram is shown in Figure 5. The light source was a hydrogen DC discharge. It consists of two water cooled brass electrodes connected by a boron nitride capillary tube. The light source was operated at 700 V and 250 ma with a gas pressure of 1-10 torr. It is attached to a two-stage differential pumping assembly which contains a set of fixed slits. This helps to reduce the pressure in the monochromator. To obtain monochromatic radiation a Seya-Namioka vacuum ultraviolet monochromator (MacPherson Model 235) was used with a Bausch and Lomb 600 lines per mm replica diffraction grating. The grating was blazed for 1500 Å and coated with aluminum to increase the reflectivity in the ultraviolet region. Two thirds of the grating was masked so that only the center section was irradiated. In order to eliminate uncertainties in the reflectance and transmission measurements due to possible instabilities in the light source a beam monitor was placed between the monochromator and the reflectance chamber (Figure 5). Approximately 50% of the incident beam struck a wedge which was coated with sodium salicylate. This phosphor emits a broad spectrum of light centered about 4200 Å when irradiated with ultraviolet light. The fluorescent radiation was then detected by an end window photomultiplier tube (EMI 9524-B) through a Pyrex light pipe which was placed in contact with the phototube with silicone jelly. The reflectance chamber was designed for studies of the optical properties of thin films

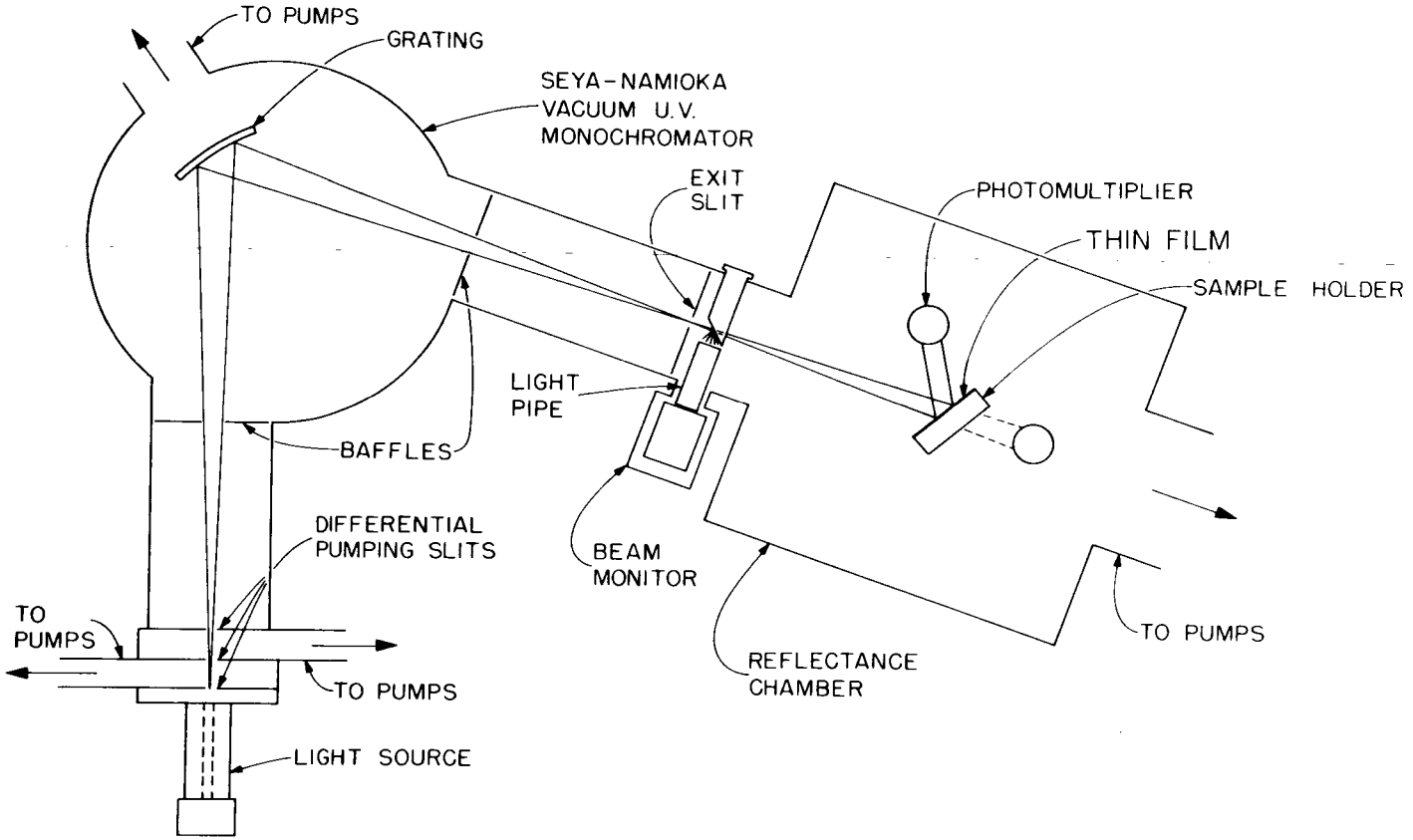


Figure 5. Schematic diagram, top view, of the experimental apparatus for measuring the optical properties.

from reflectance measurements as a function of angle of incidence and from transmission measurements at normal incidence. Most of the reflectance measurements were made at nearly normal incidence, i.e., $\theta = 20°$. When required, an angle doubler [Vehse et al. (1968)] was used to scan the reflectance as a function of angle. As the sample holder was turned, the phototube was rotated at twice the speed of rotation of the sample holder, thus enabling continuous tracking of the reflected intensity as a function of angle.

The side window photomultiplier tube (RCA 1P28) was enclosed in a stainless steel housing containing a glass window in front of the photocathode. The window was coated with sodium salicylate sprayed from an artist's airbrush to obtain a uniform film of the phosphor.

The photocurrents ranging from 10^{-7} to 10^{-10} amperes from both the reflectance chamber and the beam monitor photomultiplier tubes were measured by two picoammeters (Keithley 409). The signals were then recorded on a two-pen strip chart recorder. In addition the signals were also relayed to an analog to digital intercoupler (Beckman Model 3108) and recorded by a Teletype printer and paper tape punch. The reflectance data on tape was then directly compatible with the IBM 360 computer input.

CHAPTER IV

EXPERIMENTAL PROCEDURE AND DETERMINATION OF OPTICAL CONSTANTS

I. Substrate Cleaning

To obtain adherent and smooth coatings on glass and other substrates, the support surface must be free from contaminant films such as grease, dirt, etc. Glass and CaF_2 were used as substrates throughout the experiment. Glass slides were cleaned initially with Knox-60 Laboratory Glass Cleaner, rinsed with distilled water, then put into concentrated chromic acid to remove any soap or oil films, rinsed with distilled water thoroughly, and finally flushed with isopropyl alcohol. Since CaF_2 is slightly soluble in water, it was first washed with isopropyl alcohol, then was put into a vapor degreasing bath.

II. Film Preparation

About one hour prior to the preparation of a sample film the liquid nitrogen cold trap in the vacuum evaporator was filled. This helped to reduce the pressure of water vapor in the chamber. A thin layer of the sample which was in powdered form was put uniformly on the boat. The same tantalum boat was used throughout the experiment. It was cleaned with water and isopropyl alcohol between evaporations. The thermocouple of the temperature indicator was set on the edge of the boat at its center. The substrates were set right above the boat and the distance between boat and substrate was 12 cm. The thickness monitor was mounted at the same angle as the substrate with respect to the boat and at the same distance from the boat. Evaporations were started when the pressure

reached 6 x 10^{-6} torr. The current through the boat was raised till the evaporation rate reached its maximum. This could be determined from both the reading of the thickness monitor and the reading of the pressure. The optimum evaporation temperature for adenine was 220°C, thymine 178°C, cytosine 233°C, and guanine 355-360°C. Detailed evaporation conditions for each base are given in Table 1. In general, the evaporation rate was faster at the beginning of all the sublimations. The temperature was raised slightly within the range shown in Table 1 when the evaporation rate decreased. Because of the possibility of thermal decomposition of the nucleic acid bases, the temperatures were raised only high enough to maintain a reasonable evaporation rate.

Table 2 lists the sublimation temperatures for the four different bases we used, the sublimation temperatures Yamada and Fukutome (1968) and Johnson (1972) used, and the melting points listed in the CRC Handbook (1969). Apparently our temperatures are all much higher than those used by others. Yamada and Fukutome compared the ultraviolet absorption spectrum of the material scraped from the substrate and dissolved in phosphate buffer (pH = 7) with the absorption spectrum of the original material. The two spectra showed the same characteristics. Thus they concluded there was no thermal decomposition during the sublimation. Table 3 shows the positions of the absorption peaks for sublimed films measured in this study compared with Yamada and Fukutome's values. The agreement is good except at the shorter wavelengths. Although we did not check the thermal decomposition during the sublimation, we believe that our samples were undecomposed because of the agreement with Yamada and Fukutome's data. Besides, all the temperatures used here were lower

TABLE 1

EVAPORATION CONDITIONS FOR MAKING NUCLEIC ACID BASES FILMS

Material	Film #	Temperature (°C)	Step Thickness(es) Å	Evaporation Rate Å/hr	Substrate	Sample Vendor
Adenine	a	220-228	625,897 1099,1364	460	CaF_2	Nutritional Biochemical Corp.
	b	220-228	414,569 725,886			
	d	220-235	330,570 860,1150			
	e	220-235	4000	500	Glass	
Thymine	a	178-183	397,556 697,854	1138	CaF_2	Calbiochem. Co.
	b	178-183	457,596 744,893			
	c	178-190	1000		Glass	International Chemical

TABLE 1 (continued)

Material	Film #	Temperature (°C)	Step Thickness(es) (Å)	Evaporation Rate (Å/hr)	Substrate	Sample Vendor
Cytosine	a	233-245	360,450 540,630	210	CaF_2	Nutritional Biochemical Corp.
	b	233-236	423,583 783,1101			
	c	233-236	414,477 572,634	1100		
	f	233-245	1480		Glass	
Guanine	a	355-360	289,386 482,579	81	CaF_2	Calbiochem Co.
	b	355-360	648,565 484			Worthington Biochemical Corp.

TABLE 2

COMPARISON OF THE SUBLIMATION TEMPERATURES OF THE NUCLEIC ACID BASES

	Sublimation Temperature (°C)			M.P. (°C)
Adenine	220[a]	135[b]		360-5[d]
Thymine	178	150		326
Guanine	355-360	290	200[c]	360
Cytosine	233	180	90	320-25

[a] Present work.

[b] Yamada and Fukutome (1968).

[c] Johnson (1972).

[d] CRC Handbook (1969).

TABLE 3

COMPARISON OF THE ABSORPTION PEAKS FOR SUBLIMED NUCLEIC ACID BASES FILMS

Material	Present Work (Å)	Yamada and Fukutome (1968) (Å)
Adenine	2715	2690-2720
	2060	2100
	1830	1820
	1600	1600
	1425	1450*
		1400
Thymine	2750	2650-2700
	2630	
	2100	2110
	1790	1760
	1600	1600*
	1440	1520*
	1375	1440
Cytosine	2720	2700-2710
	2025	1990-2030
	1620	1610
	1510	1500
		1420*
Guanine	2820	2820-2890
	2545	2460-2510
	2000	1980-2000
	1875(s)	1850
	1560	1550*
	1390	1430*

(s) Shoulder.

Peaks marked by "" are poorly resolved and are not regarded as certainly established.

than the decomposition temperatures listed in the CRC Handbook except for guanine. Although we tried the temperatures given by Yamada and Fukutome, no appreciable evaporation was found at the temperatures they listed.

Films of four different thicknesses were made side by side on the same CAF_2 substrate for transmission measurements. A shutter set right below the substrate was attached to a rod that could be rotated outside the coating chamber. When a certain desired thickness was obtained, the shutter was rotated to a position so that one fourth of the width of the substrate was covered. When the next desired thickness was reached, another one fourth of the width of the substrate was covered. In this way, four different thickness films were made on one CaF_2 substrate. Only one film thickness was made on each glass slide for reflectance measurements. At least two different films were made for each base to check on consistency. Measurements for thickness were also made by optical interferometry, to check the accuracy of the quartz crystal thickness monitor, for films of adenine. A thin silver film was coated on the edge of the sample films. Sodium light with wavelength 5890 Å was used as the incident light. When the Fizeau flat is brought in contact with a reflecting sample in such a way that a thin air wedge is established, a series of parallel lines representing constructive and destructive interference were obtained. The horizontal spacing between these parallel lines represents 1/2 wavelength of the incident light. Any displacement of the parallel lines denotes a change in surface elevation. By measuring the ratio

of the step height to the fringe spacing (i.e., 2945 Å), one can determine the step height and thus the film thickness. The difference between the readings from the thickness monitor and the interferometer was less than 5% of either.

III. Transmission Measurements

Transmission measurements were made immediately after the samples were moved to the reflectance chamber. Since CaF_2 transmits light above 1200 Å, it is a good substrate for measuring the transmitted light above 1200 Å. The experimentally measured transmission, T, is

$$T = \frac{I}{I_o} \tag{44}$$

where I_o is the intensity for the incident light and I is the intensity for the transmitted light. From Equation (31)

$$T = \frac{I}{I_o} = e^{-\frac{4\pi kd}{\lambda}} . \tag{45}$$

The relative transmitted light intensity as a function of thickness on a semi-log plot should be a straight line with the slope yielding the value of k (Figure 6). Corrections for background radiation resulting from the dark current of the photomultiplier and scattered light were made on each step of the film in the wavelength region just below the cut-off of the filter used. Filters were used to eliminate the second and higher orders of diffraction. In the region 1600 Å to 3000 Å, a quartz filter was used, in the region 1200 Å to 1600 Å, no filter was used, since the CaF_2 substrate acted as a filter. Sometimes because of the change in scale when making transmission measurements or because of some other unknown reasons, only three points fell on a

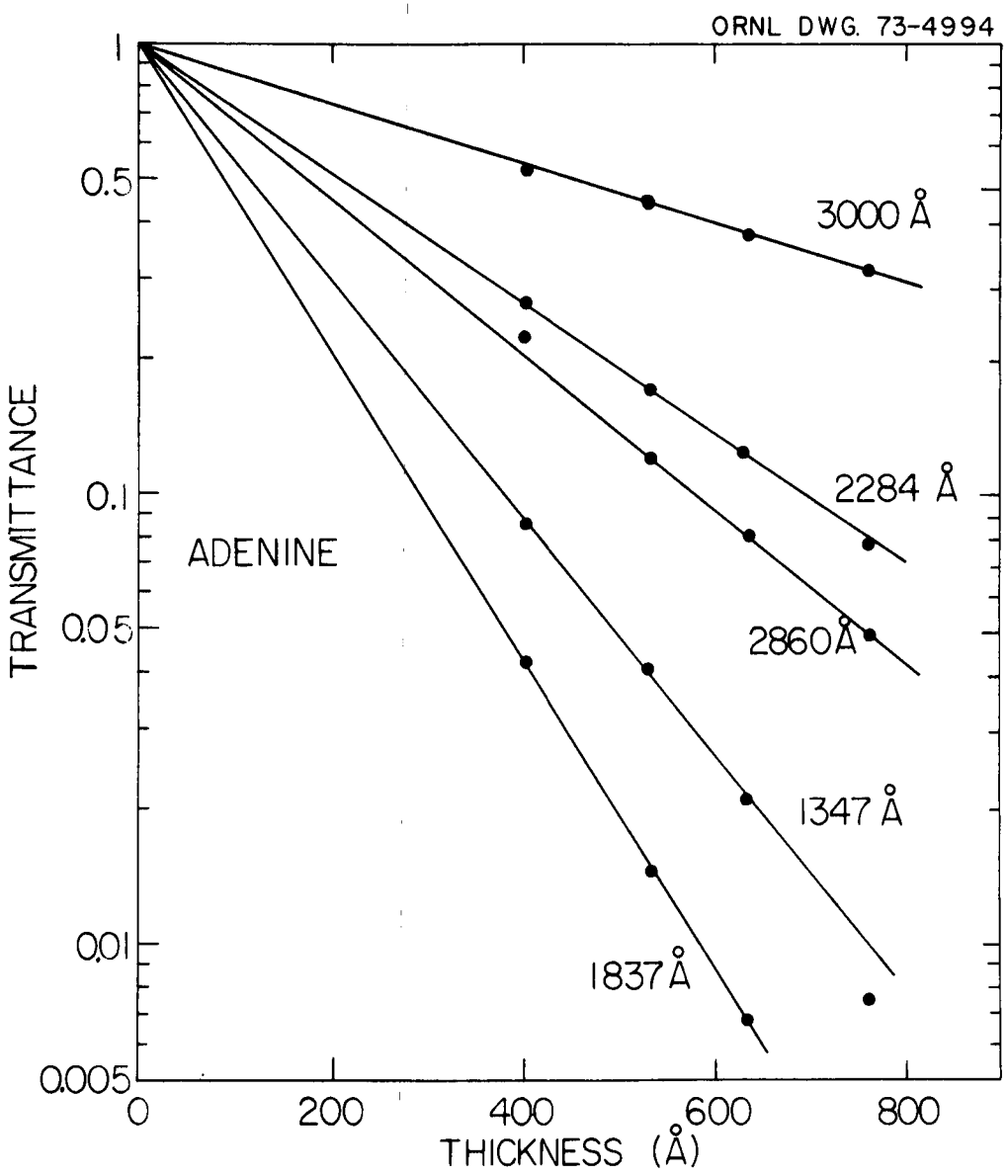


Figure 6. Transmission of adenine from films of four different thicknesses.

straight line. The point off the line was neglected. In addition, transmission was obtained by using one thickness of the film and scanning wavelength for both I and I_o. In this way, the relative structure in k as a function of wavelength can be obtained. This was done for guanine and cytosine. All the nucleic acid bases spectra become transparent in the region above 3500 Å. If there is apparent absorption above 3500 Å due to surface or bulk scattering from the films, corrections to the data must be made [Yamada and Fukutome (1968)].

Scattered light from the films used in this study was negligible throughout the whole experiment. This was verified as follows: in the region above 3500 Å, the transmitted light intensities for different steps on one substrate became nearly the same, i.e., the difference in intensity was not greater than 2%. Even if the transmitted light intensities were not the same, the slope of the plot of the transmitted light intensities versus thickness was negligible compared with the values obtained in the regions of high absorption.

IV. Reflectance Measurements

Reflectance measurements were made at nearly normal incidence from the films sublimed on glass slides. The reflectance was obtained from the expression

$$R(\theta) = \frac{I(\theta)}{I_o} \tag{46}$$

where I_o is the incident light intensity and $I(\theta)$ is the reflected light intensity at angle θ. The reflectance measurements were made at $\theta = 20°$ for the four bases in this experiment. Corrections for the background

radiation were the same as for the transmission measurements. By measuring R at $\theta = 20°$ and using the k value from the transmission measurements, the index of refraction, n, can be calculated. This was done by putting the appropriate values of R and k together with the corresponding thickness, d, index of refraction for the media on either side of the film, n_o and n_2, and the polarization, P, at each wavelength used into Equations (12) through (30). The polarization was measured with a triple-reflection polarizer [Horton et al. (1969)] from 500 Å to 3000 Å and with Polaroid HN-22 from 2800 Å to 6000 Å.

CHAPTER V

RESULTS AND DISCUSSION

I. Optical Constants

The extinction coefficients, k, as a function of wavelength for the four nucleic acid bases are shown in Figures 7 through 10. Unless otherwise specified, the k value was calculated from the transmission of the corresponding films listed in Table 1, page 26. Curves d and e of cytosine were calculated from measurements of the transmission of the step with thickness 477 Å of film c. Curves b, c, and d of guanine were the k values calculated from the transmission of steps with thickness 648, 565, and 484 (Å) of film b, respectively. The cut-off wavelength was determined from the wavelength at which transmission from different thicknesses became the same.

The index of refraction, n, was calculated from the reflectance at $\theta = 20°$ and the k value obtained from the transmission measurements. The reflectances, R, at $\theta = 20°$ and the indices of refraction, n, as a function of wavelength are shown in Figures 11 through 14. All the reflectances were measured from the films on glass slides except for guanine. For guanine, the reflectance was obtained from the step with thickness 648 Å of film b.

The index of refraction was calculated from the solid lines of R and one set of k values; for adenine, curve d, for thymine, curve a, for cytosine, curve d, and for guanine, curve b.

All the long dashed lines for the index of refraction in the transparent region for adenine, cytosine, and guanine were obtained by Abeles'

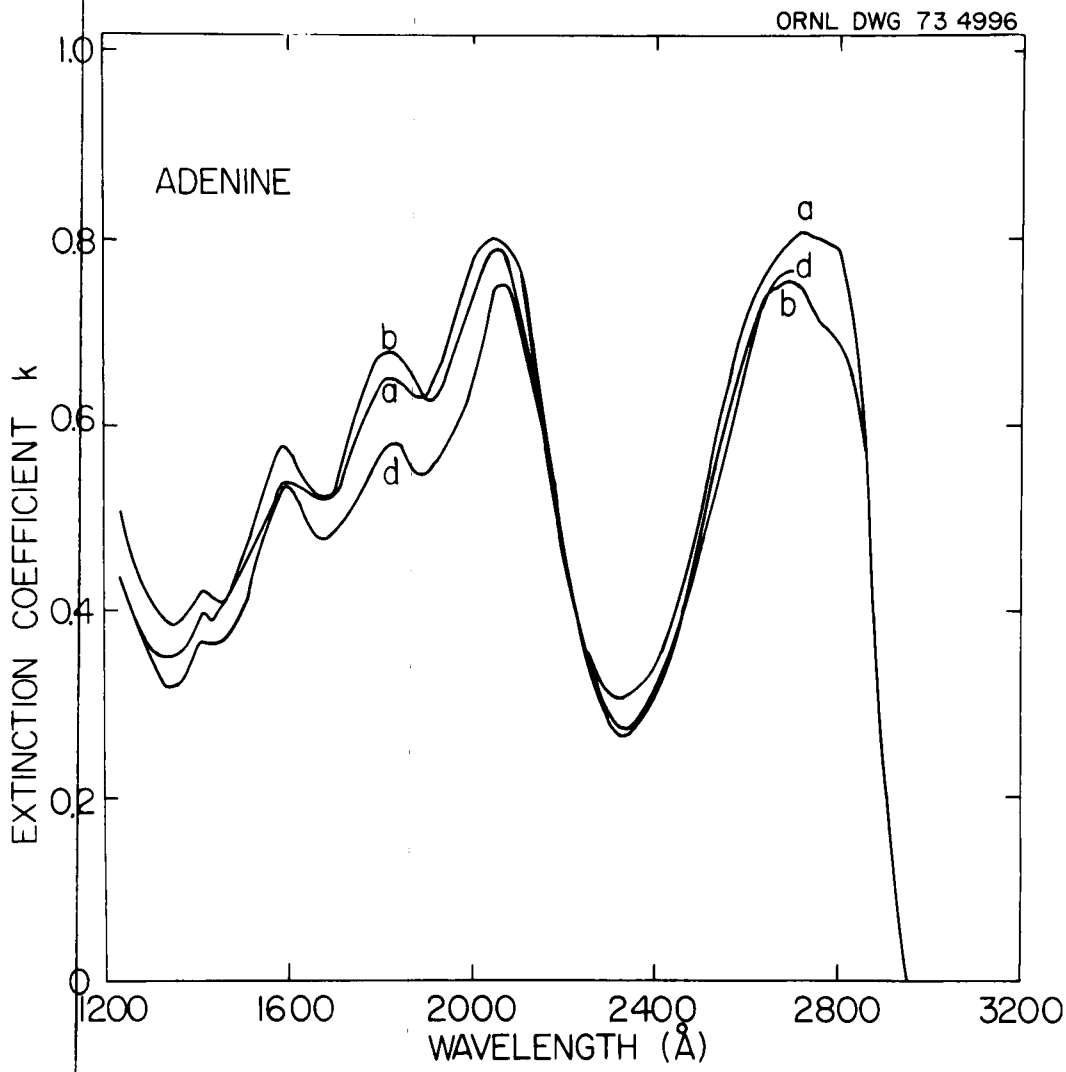


Figure 7. Extinction coefficient, k, of adenine as a function of wavelength.

(For an explanation of curves a, b, and d, refer to Chapter V, p. 35.)

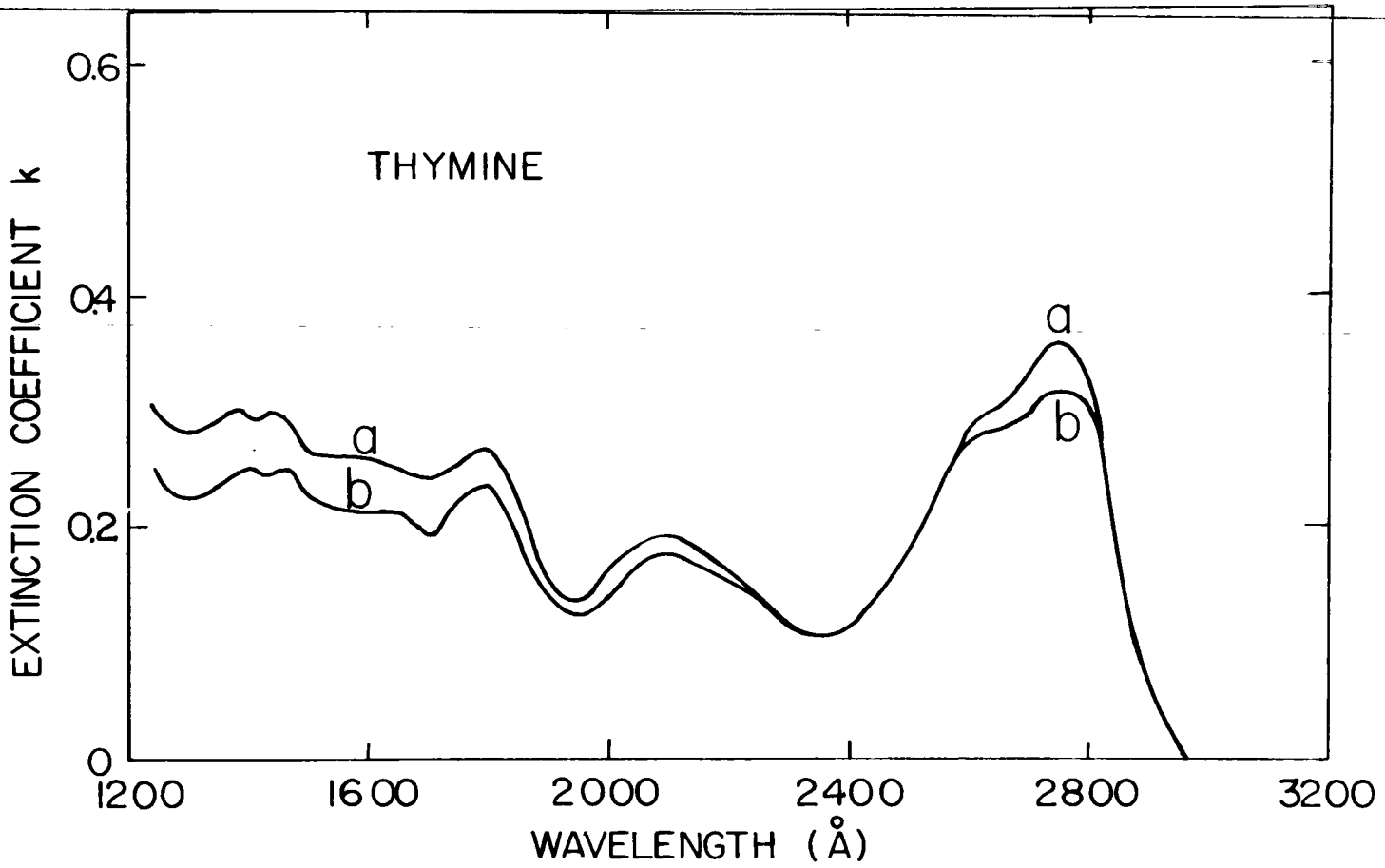


Figure 8. Extinction coefficient, k, of thymine as a function of wavelength.

(For an explanation of curves a and b, refer to Chapter V, p. 35.)

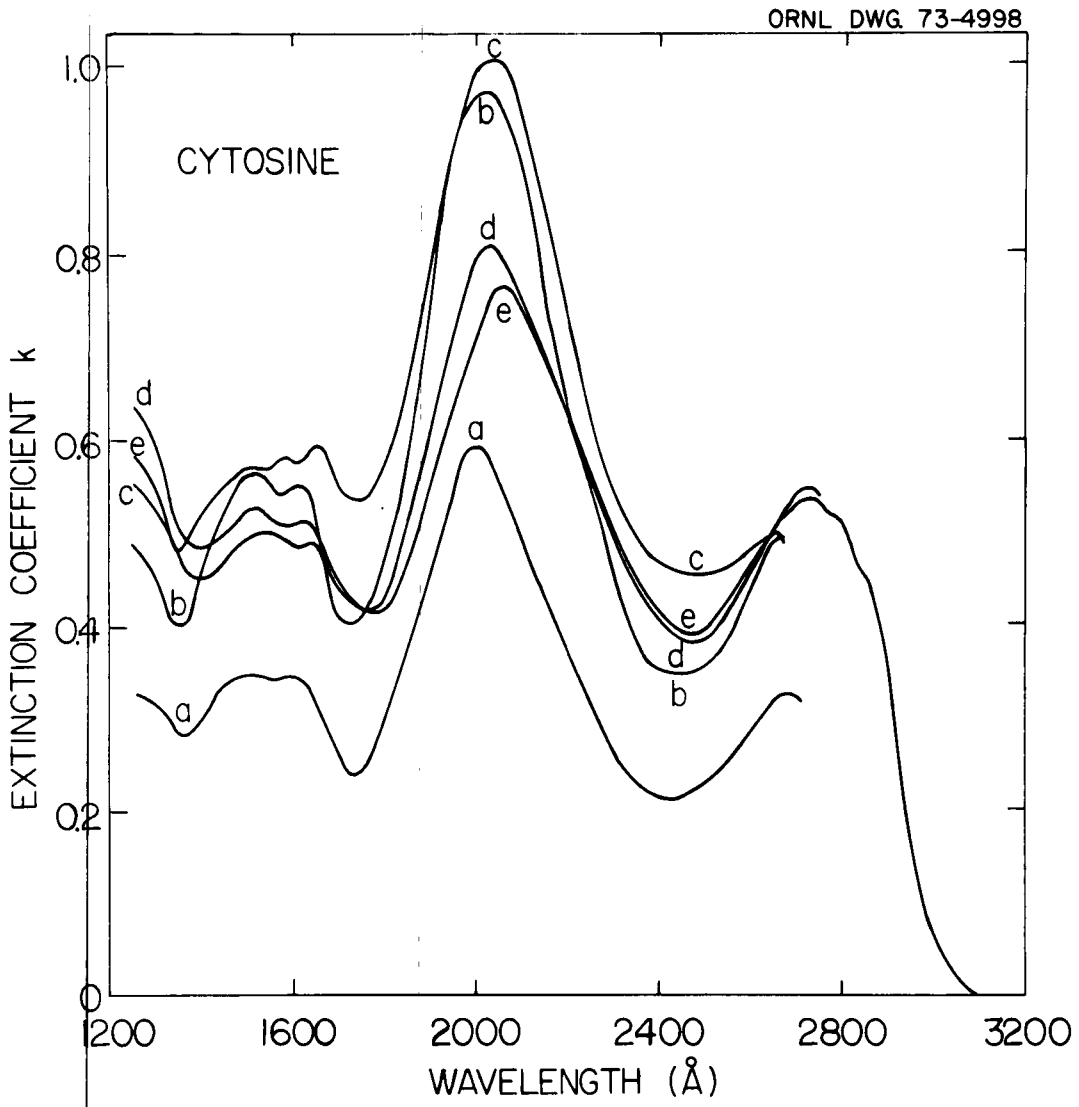


Figure 9. Extinction coefficient, k, of cytosine as a function of wavelength.

(For an explanation of curves a, b, c, d, and e, refer to Chapter V, p. 35.)

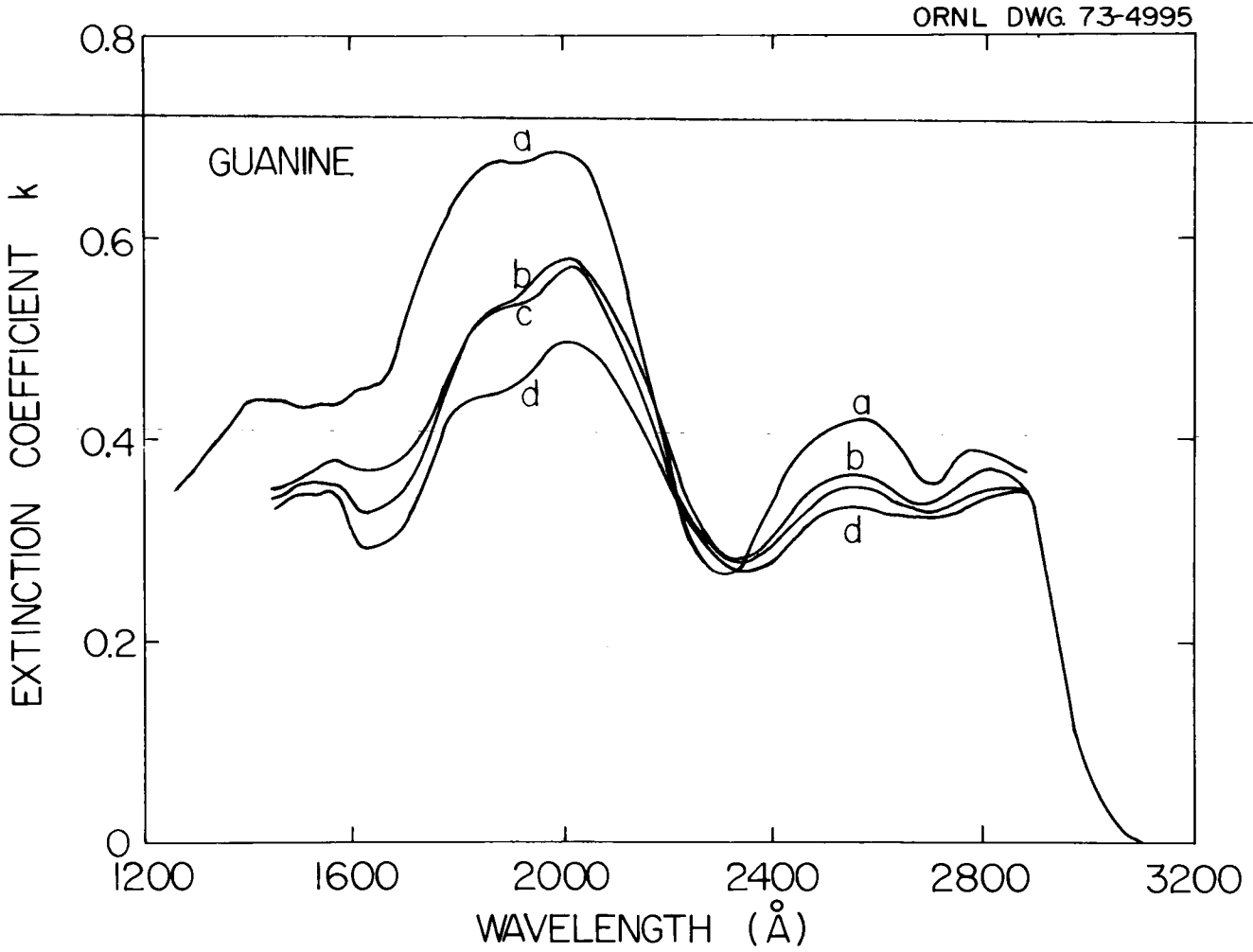


Figure 10. Extinction coefficient, k, of guanine as a function of wavelength.

(For an explanation of curves a, b, c, and d, refer to Chapter V, p. 35.)

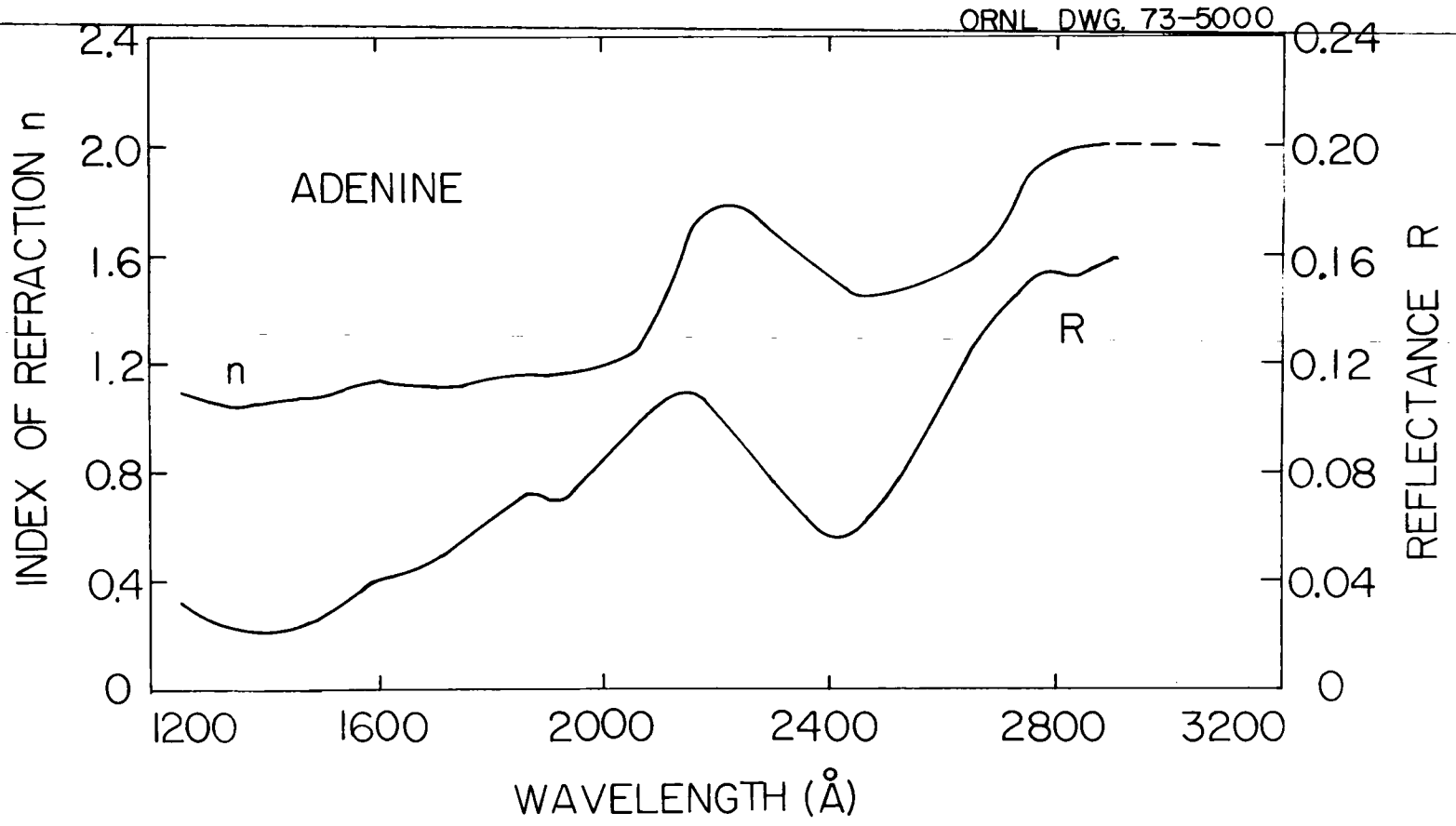


Figure 11. Reflectance, R, and index of refraction, n, of adenine as a function of wavelength.

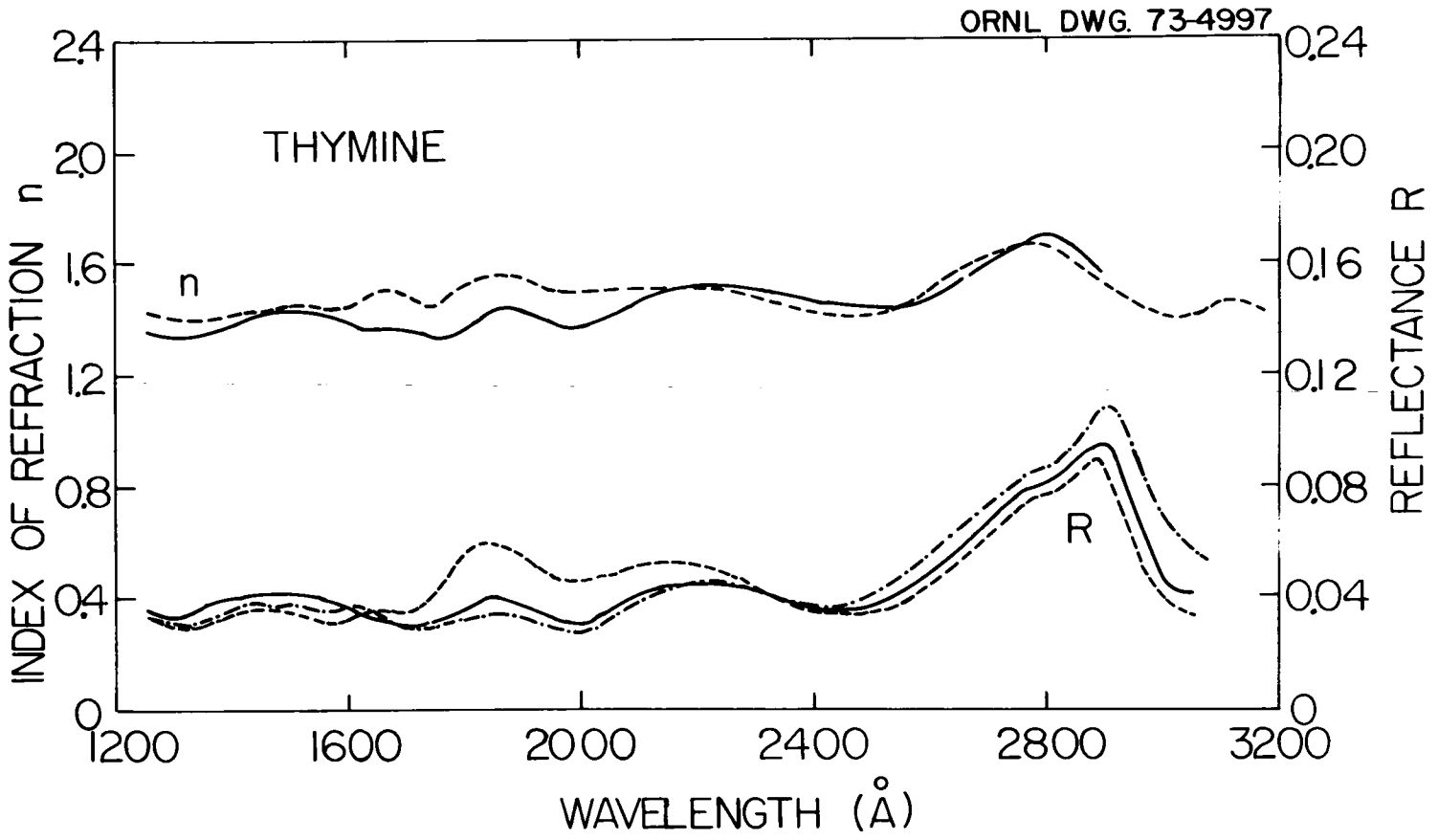


Figure 12. Reflectance, R, and index of refraction, n, of thymine as a function of wavelength.

(The three reflectance curves are measurements on the same film taken at different times; --- n value from R vs. θ analysis.)

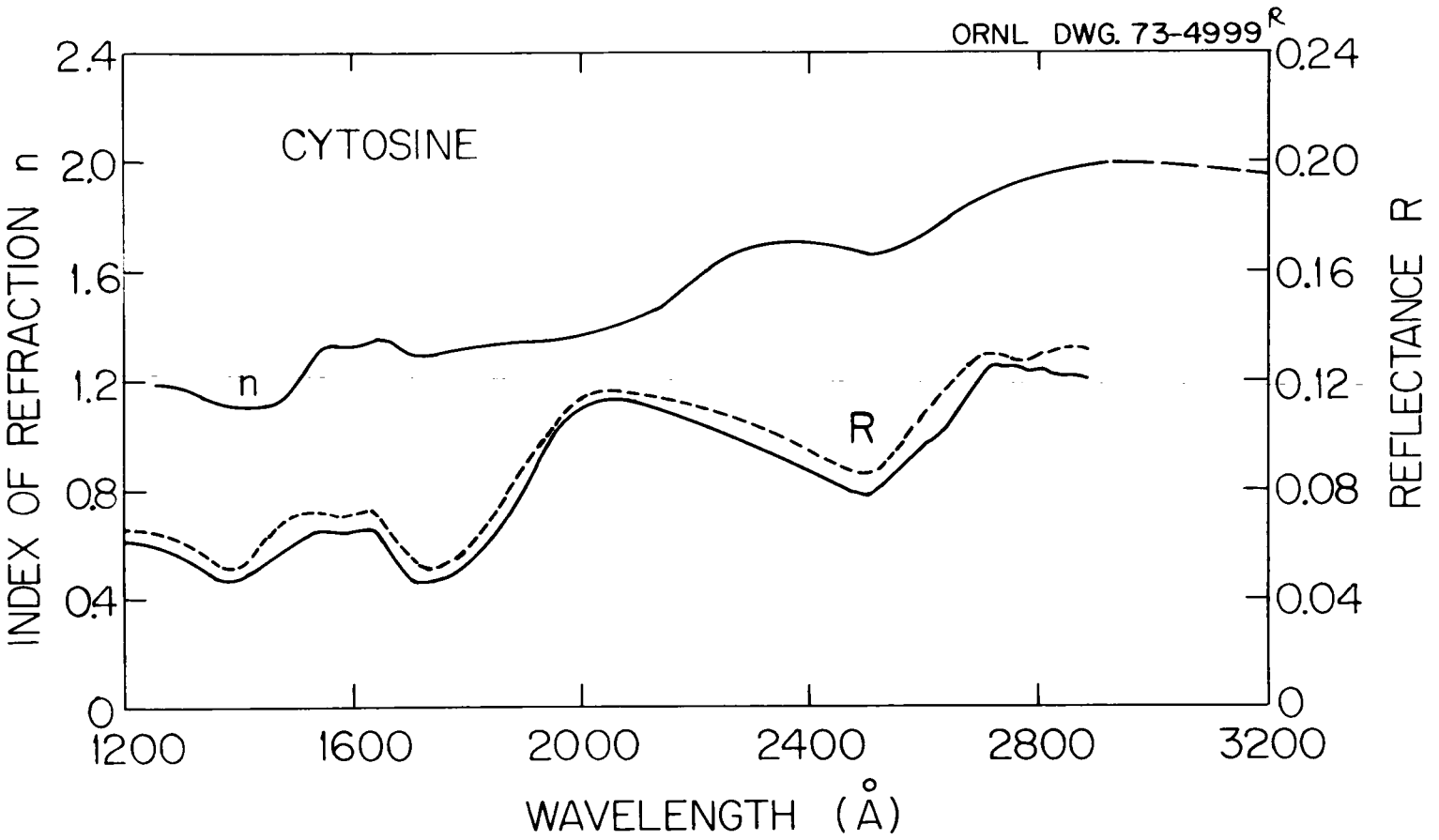


Figure 13. Reflectance, R, and index of refraction, n, of cytosine as a function of wavelength.

(The two reflectance curves are measurements on the same film taken at different times.)

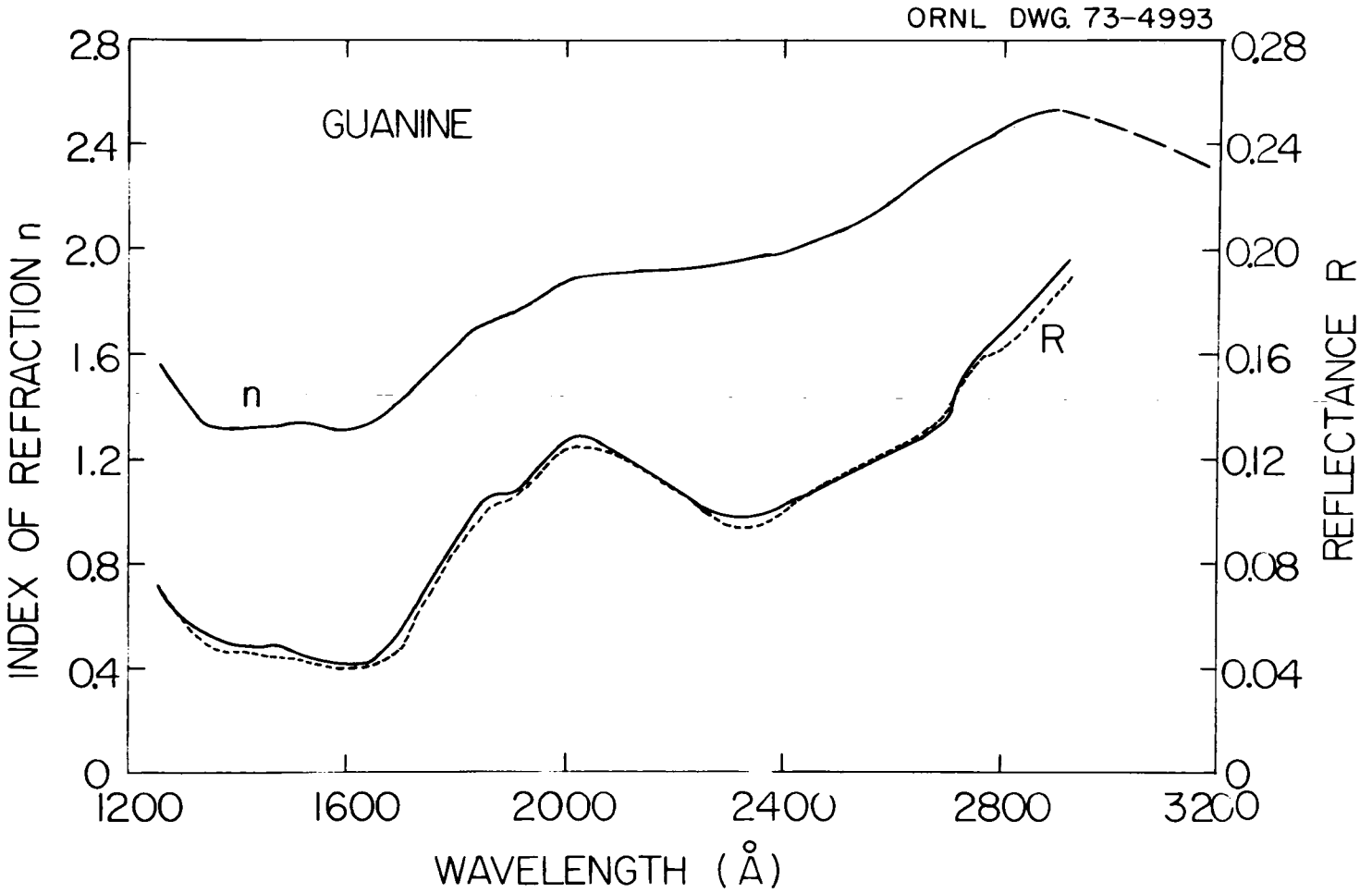


Figure 14. Reflectance, R, and index of refraction, n, of guanine as a function of wavelength.

(The two reflectance curves are measurements on the same film taken at different times.)

method [Heavens (1965)]. There is little doubt in the structure of the k values obtained from the transmission method for each film, but the magnitude of k is not reproducible from one film to another, especially in the shorter wavelength range. The factors governing this are not understood yet. The smoothness of the film becomes very important in the short wavelength region of the spectrum. Inhomogeneities in the films, surface irregularities, and contamination of the film could be some of the factors involved. Detailed experimentation on conditions affecting film structure such as the determination of the appropriate evaporation method, optimum distance between the source and the substrate, optimum temperature and hence the rate of sublimation, etc., still has to be done. The index of refraction, n, was calculated from representative sets of R and k values. These n and the corresponding k values were then used to calculate the dielectric constants, ε_1 and ε_2, and the energy loss function, $-\mathrm{Im}(1/\varepsilon)$.

II. Optical Properties

The dielectric constants, ε_1 and ε_2, and the energy loss function, $-\mathrm{Im}(1/\varepsilon)$, together with the data from the electron energy loss as a function of energy for the four bases are shown in Figures 15 through 18.

Several things must be taken into consideration when comparing optical spectra with the corresponding energy loss spectra [Powell (1969)]. Since the optical constants $n(\omega)$ and $k(\omega)$ are related to the complex dielectric constant $\varepsilon(\omega,\vec{k} = 0)$, the energy loss function $-\mathrm{Im}[1/\varepsilon(\omega,0)]$, calculated from the optical data corresponds to a "zero-angle" electron energy loss spectrum. If the extent of the experimental angular integration has not been adequately specified, such spectra cannot be compared

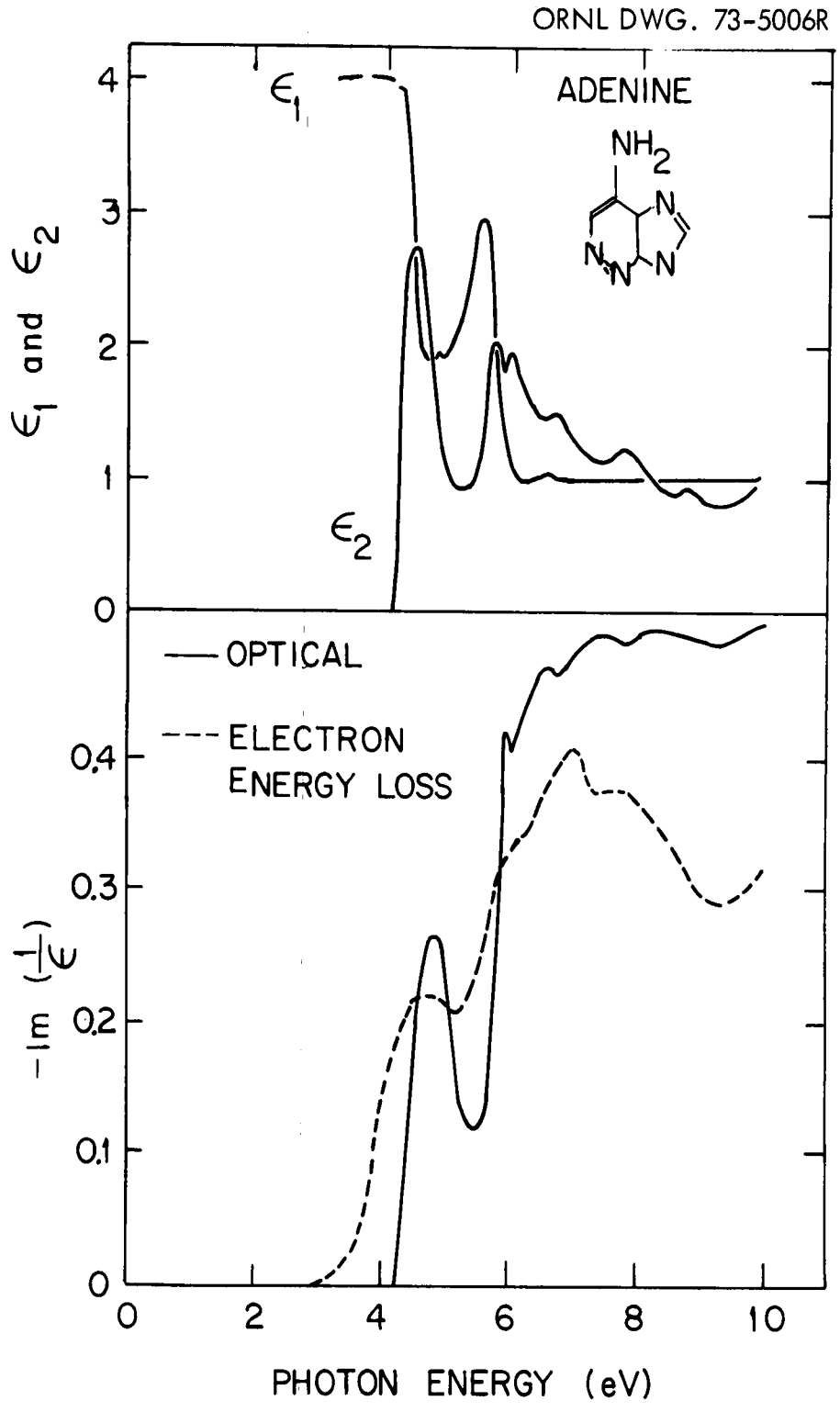


Figure 15. Dielectric constant,. ε_1 and ε_2, and energy loss functions, $-\mathrm{Im}(1/\varepsilon)$, of adenine as a function of photon energy.

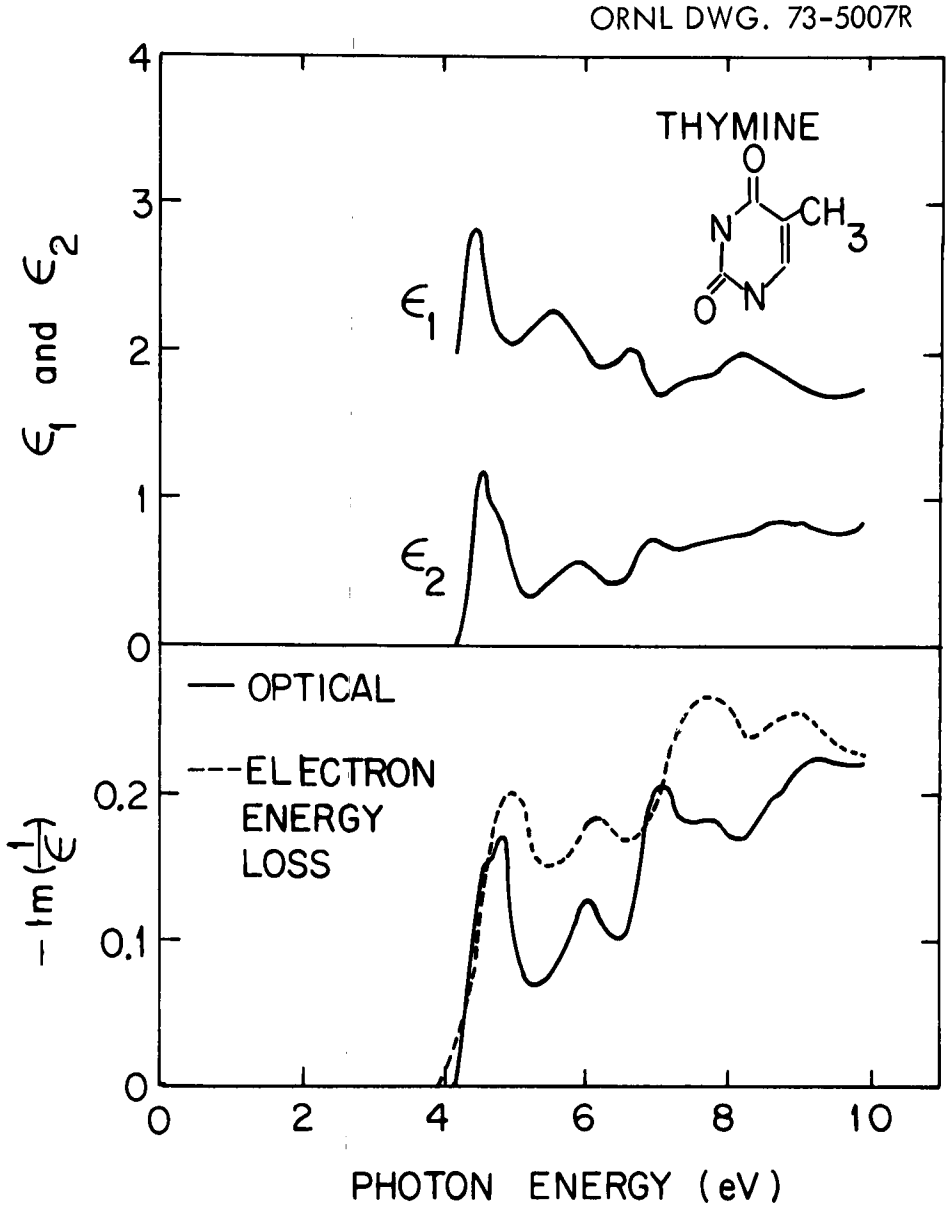


Figure 16. Dielectric constants, ε_1 and ε_2, and energy loss function, $-\mathrm{Im}(1/\varepsilon)$, of thymine as a function of photon energy.

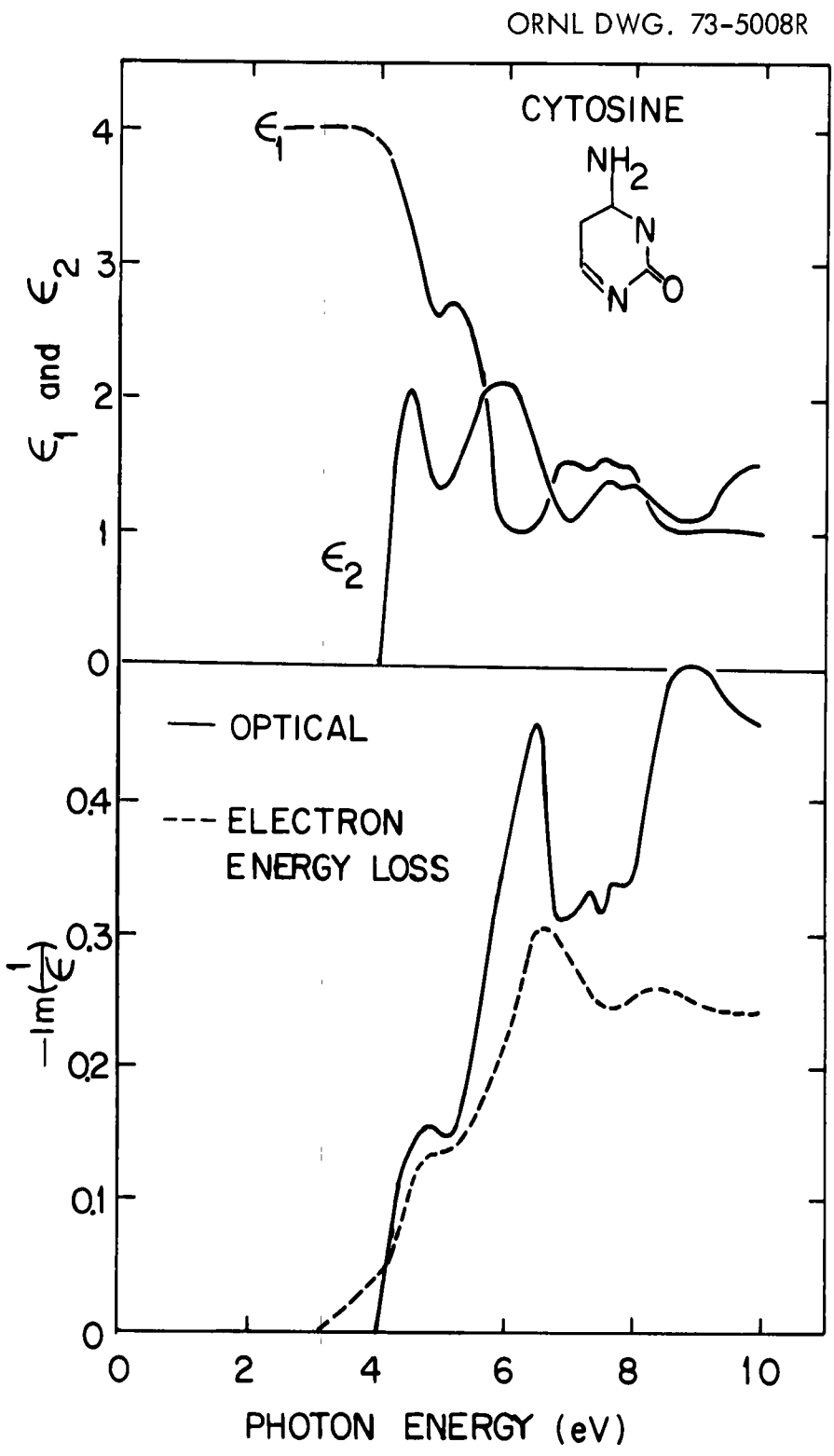


Figure 17. Dielectric constants, ε_1 and ε_2, and energy loss function, $-\mathrm{Im}(1/\varepsilon)$, of cytosine as a function of photon energy.

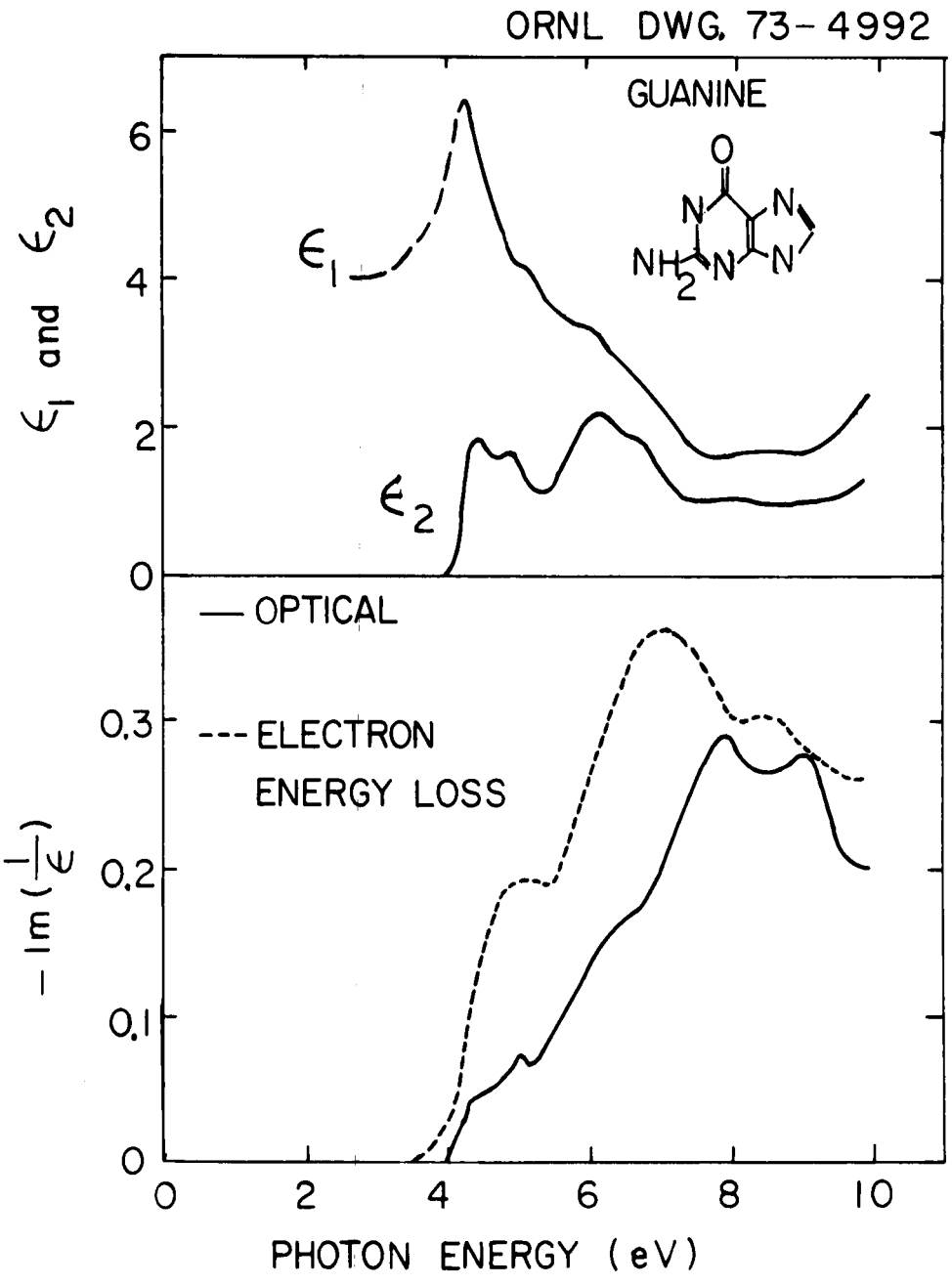


Figure 18. Dielectric constants, ε_1 and ε_2, and energy loss function, $-\mathrm{Im}(1/\varepsilon)$, of guanine as a function of photon energy.

in detail with $\mathrm{Im}[1/\varepsilon(\omega,0)]$. In addition, corrections due to multiple inelastic scattering and to the excitation of multiple plasmon losses must be made when it is desired to determine $\mathrm{Im}[1/\varepsilon(\omega,0)]$ from transmission energy loss spectra. Optimum specimen thickness should be chosen to minimize these corrections.

Creuzburg et al. (1964) compared the electron energy loss spectra of KCl and KBr with optically measured spectra of $\mathrm{Im}(1/\varepsilon)$. Good agreement was found in both the position of the peaks and in the general shape. Raether (1968) compared the electron energy loss spectra of Al, Ge, GaP, and KBr with the optically determined loss spectra. Good agreement was found in both the position of the peak and the absolute intensity for Al, and in the general shape and the positions of the peaks for Ge, GaP, and KBr.

In the electron energy loss experiments for nucleic acid bases [Johnson (1972) and Isaacson (1972], the incident beam aperture and the analyzer aperture subtended a half angle of 0.625 mrad. This aperture size was approximately equal to, or smaller than, the characteristic inelastic angle $\theta_E = E/2E_o$ for all energy losses E. This could be considered as a zero-angle electron energy loss distribution. Corrections were made only for double inelastic scattering. For the film thickness and experimental apparatus they were using, triple and higher order inelastic scattering could be neglected. These corrections enable us to compare directly with the loss spectra from our optical measurements. It is seen that the general shapes of the energy loss functions from the optical method are similar to those of the electron energy loss. Table 4 gives a comparison of the peaks in $-\mathrm{Im}(1/\varepsilon)$ from both electron energy

TABLE 4

COMPARISON OF THE POSITIONS OF THE PEAKS IN $-Im(1/\varepsilon)$ FROM BOTH ELECTRON ENERGY LOSS AND OPTICAL MEASUREMENTS, IN ε_2 AND IN THE ABSORPTION COEFFICIENT μ FOR SUBLIMED FILMS

$-Im(1/\varepsilon)$ (eV)		ε_2	μ
Electron Energy Loss	Optical (this paper)	Optical (this paper)	Absorption Coefficient (eV)
		A. Adenine	
4.75[a]	4.79	4.50	4.58[b]
6.0[s]	5.90	5.81	5.90
6.9	6.55	6.74	6.80
	7.45		
7.71		7.80	7.74
	8.35	8.75*	
		B. Thymine	
	4.53[s]	4.53	4.63[b]
4.89[a]	4.80		
6.10	6.0	5.90	5.86
7.70	7.0	6.90	7.04
	7.75[s]		
	8.65[s]	8.65	8.60
8.9		9.01(small)	
	9.2		
		C. Cytosine	
		4.52	4.58[b]
4.83[c]	4.83	5.91	6.15
	6.51		
6.53	7.53		
	7.69	7.6	7.70
8.5	8.89	8.0	8.27

TABLE 4 (continued)

-Im(1/ε) (eV)		ε_2	μ
Electron Energy Loss	Optical (this paper)	Optical (this paper)	Absorption Coefficient (eV)
		D. Guanine	
	4.35(s)	4.4	4.38(b)
5.0(c)	4.96	4.83	4.96
	6.55(s)	6.15	6.23
7.05	7.87	8.0	8.0
8.5			
	9.0	8.95	

(a) Isaacson (1972).

(b) Yamada and Fukutome (1968).

(c) Johnson (1972).

(s) shoulder.

loss and optical measurements, in ε_2 from optical measurements and in the absorption coefficient, μ, obtained from the literature [Yamada and Fukutome (1968)].

The analysis presented so far has shown that the loss functions calculated from optical measurements on thin films of the nucleic acid bases can be compared directly with electron energy loss spectra reported in the literature. Since difficulties were experienced with film reproducibility and "representative" values of k and R were used to calculate n and hence ε_1, ε_2, and $-\mathrm{Im}(1/\varepsilon)$, we cannot attempt a detailed analysis of the results presented in Figures 15-18, pages 45-48. No real significance can be attached to the differences in magnitude of the loss functions calculated from electron losses and from the optical measurements, or to the differences in peak energies tabulated in Table 4. It is, however, significant that even with the uncertainties in k, the overall structures seen in Figures 15-18 in $-\mathrm{Im}(1/\varepsilon)$ by the two methods are similar and that the present optical method yields a higher resolution than the electron energy loss measurements.

Isaacson (1972) and Johnson (1972) have interpreted peaks in the calculated optical absorption occurring in the energy region of our measurements in terms of $\pi \rightarrow \pi^*$ and $\sigma \rightarrow \sigma^*$ molecular transitions. They also find that peaks in the energy loss spectra are shifted to energies higher than the corresponding optical transitions. The magnitude of this shift gives some qualitative indication of the degree of collective effects associated with a particular peak although it does not permit one to say how much of a particular transition is "collective" or "non-collective" in nature. Structure in $-\mathrm{Im}(1/\varepsilon)$ was shown to correspond

to the same optical transitions seen in the absorption with the peaks in $-\mathrm{Im}(1/\varepsilon)$ shifted to higher energies. The energy loss functions were then interpreted in terms of collective effects associated with the molecular excitations. These collective effects are hybrid resonances rather than the totally free electron resonances seen in nearly-free-electron-like metals. However, both the hybrid and nearly-free-electron resonances occur when the magnitudes and energy variations of the dielectric functions show similar properties suitable for sustaining collective oscillations (see Chapter II, page 17).

It is felt that the interpretations given by Isaacson and Johnson are substantially correct. When the problems associated with film preparation have been solved, the higher resolution of the optical measurements may allow a more precise determination of molecular excitations and resonance energies. It should also be possible to estimate whether the electron energy loss measurements do actually produce sufficient radiation damage to alter the spectra. When problems have been solved in the low energy region it is proposed to extend the observations up to $\sim$80 eV using a soft x-ray grazing incidence monochromator.

CHAPTER VI

SUMMARY

The optical properties of the nucleic acid bases, adenine, thymine, cytosine, and guanine, were studied in the energy range from 4 to 10 eV. Thin films of these bases were vacuum-deposited on CaF_2 or glass for transmittance and reflectance measurements. Different evaporation conditions such as sublimation temperature, evaporation rate, etc., were used for different bases. Transmittance and reflectance measurements were made immediately after the films were transferred into the reflectance chamber. The extinction coefficient, k, was determined from the transmission measurements. The positions of the absorption peaks agree fairly well with the previous work. The magnitude of the k value differs from one film to another. The factors governing the reproducibility could be the inhomogeneities in the films, surface irregularities, and contaminations involved. More work has to be done on film preparation. The reflectance measurements were made at 20 degrees angle of incidence. The index of refraction, n, was calculated from representative sets of R and k. The complex dielectric constants, $\varepsilon = \varepsilon_1 + i\varepsilon_2$, and the energy loss functions, $-\mathrm{Im}(1/\varepsilon)$, were then calculated from these n and the corresponding k values. The energy loss functions were compared with those from electron beam experiments. Since only representative sets of R and k were used to calculate n and hence ε_1, ε_2, and $-\mathrm{Im}(1/\varepsilon)$, no real significance is attached to the differences in the magnitude of the energy loss functions calculated from electron energy loss and the optical measurements. However, the

overall structures from these two different methods are similar and the present optical method has a higher resolution than the electron energy loss method. The absorption peaks in this energy range were interpreted as $\pi \rightarrow \pi^*$ and $\sigma \rightarrow \sigma^*$ molecular transitions by Isaacson (1972) and Johnson (1972). Structures in $-\mathrm{Im}(1/\varepsilon)$ correspond to the same molecular excitations hybridized with collective effects. The shift in the positions of the peaks of the energy loss functions from the absorption peaks gives some qualitative indication of the degree of collectivity associated with a particular molecular transition.

When the problems in film preparation are solved, the optical method will enable us to have a more precise determination of molecular excitation and resonance energies. It is proposed to extend the present work up to $\sim$80 eV using a soft x-ray grazing incidence monochromator.

BIBLIOGRAPHY

BIBLIOGRAPHY

Creuzburg, M. and H. Raether, Solid State Communication 2, 345 (1964).

Ehrenreich, H., and H. R. Phillips, in Proceedings of the International Conference of the Physics of Semiconductors, ed. by A. C. Strickland (Bartholomew Press, Dorking, England 1962), pp. 367-374.

Fenton, E. W., Phys. Rev. 174, 517 (1968).

Handbook of Chemistry and Physics, ed. by R. C. Weast (Chemical Rubber Publishing Company, Cleveland, Ohio 1969-1970), 50th ed., pp. C-97, C-263, C-318, and C-512.

Heavens, O. S., Optical Properties of Thin Solid Films (Dover Publications, Inc., New York 1965), pp. 119-153.

Hoffman, T. A. and J. Ladik, in "The Structure and Properties of Biomolecules and Biological Systems," Vol. VII of Advances in Chemical Physics, ed. by J. Duchesne (John Wiley and Sons, New York 1964).

Horton, V. G., E. T. Arakawa, R. N. Hamm, and M. W. Williams, Applied Optics 8, 667 (1969).

Isaacson, M., J. Chem. Phys. 56, 1803 (1972).

Johnson, D. C. Rad. Res. 49, 63 (1972)

Kloos, T., Z. Phys. 210, 303 (1968).

Ladik, J., Int. J. Quantum Chem. 4, 307 (1971).

O'Konski, C. T., P. Moser, and M. Shirai, Biopolymers 1, 479 (1964).

Powell, C. J., J. Opt. Soc. Am. 59, 738 (1969).

Pullman, B and A. Pullman, Prog. in Nucleic Acid Res. and Molec. Biol. 9, 327 (1969)

Raether, H., Helvetica Physica Acta 41, 1112 (1968).

Rhodes, W., J. Am. Chem. Soc. 83, 3609 (1961).

Ritchie, R. H., Phys. Rev. 106, 874 (1957).

Snart, R. S. Biopolymers 6, 293 (1968).

Vehse, R. C., J. C. Sutherland, and E. T. Arakawa, Rev. Sci. Instr. 39, 268 (1968).

Voet, D., W. B. Gratzer, R. A. Cox, and P. Doty, Biopolymers 1, 193 (1963).

Watson, J. D., and F. H. C. Crick, in Fundamentals of Physical Science (McGraw-Hill, Inc., New York 1971), 6th ed., pp. 568-570.

Weissbluth, M., Quarterly Rev. of Biophys. 4, 1 (1971).

Yamada, T., and H. Fukutome, Biopolymers 6, 43 (1968).

VITA

I-lan Tang was born in Taiwan, Republic of China, on October 20, 1949. She attended Taipei First Girls' School and was enrolled at Tung-Hai University in 1967. She was awarded a Bachelor Degree of Science with a major in Physics in 1971. She then attended the University of Tennessee at Knoxville majoring in Physics. She was employed as a Graduate Assistant during her graduate studies.